
DEEP-MACROFIN: INFORMED EQUILIBRIUM NEURAL NETWORK FOR CONTINUOUS TIME ECONOMIC MODELS

Yuntao Wu

Electrical and Computer Engineering
University of Toronto
Toronto, Ontario, Canada
winstonyt.wu@mail.utoronto.ca

Jiayuan Guo

Joseph L. Rotman School of Management
University of Toronto
Toronto, Ontario, Canada
flora.guo@mail.utoronto.ca

Goutham Gopalakrishna

Joseph L. Rotman School of Management
University of Toronto
Toronto, Ontario, Canada
goutham.gopalakrishna@rotman.utoronto.ca

Zisis Poulos

School of Information Technology
York University
Toronto, Ontario, Canada
zpoulos@yorku.ca

August 19, 2024

ABSTRACT

In this paper, we present Deep-MacroFin, a comprehensive framework designed to solve partial differential equations, with a particular focus on models in continuous time economics. This framework leverages deep learning methodologies, including conventional Multi-Layer Perceptrons and the newly developed Kolmogorov-Arnold Networks. It is optimized using economic information encapsulated by Hamilton-Jacobi-Bellman equations and coupled algebraic equations. The application of neural networks holds the promise of accurately resolving high-dimensional problems with fewer computational demands and limitations compared to standard numerical methods. This versatile framework can be readily adapted for elementary differential equations, and systems of differential equations, even in cases where the solutions may exhibit discontinuities. Importantly, it offers a more straightforward and user-friendly implementation than existing libraries.

1 Introduction

Partial Differential Equations (PDEs) represent a class of mathematical equations that encapsulate rates of change with respect to continuous variables. These equations are ubiquitous in the fields of physics and engineering, offering succinct insights into phenomena pertaining to acoustics, thermodynamics, and electrodynamics, etc, where closed-form analytical solutions may not always be found. In the realm of macroeconomics and finance, PDEs are used to model and forecast complex phenomena like economic growth, inflation, interest rates, and asset prices. General equilibrium problems in these fields are typically governed by non-linear parabolic PDEs [7, 6, 1, 13]. The ability to numerically solve PDE systems empowers us to scrutinize the effects of parameter alterations on the equilibrium state.

Given the inherent complexity in deriving exact analytic solutions to PDEs, particularly for nonlinear PDE problems, researchers frequently resort to numerical techniques, such as the Finite Difference Method (FDM) [16, 5], the Finite Element Method (FEM) [34, 29], and the Boundary Element Method [2]. The fundamental concept behind these numerical solutions involves discretizing the continuous domain into a grid (mesh) of finite elements and approximating derivatives using differences between adjacent points. While these methods can yield accurate solutions within a short simulation with careful grid choices, they may encounter instability and high computational costs, particularly for higher-dimensional problems or complex physical systems [17, 20]. D’Avernas et al. demonstrate that standard FDM can break down when solving economic problems, even with just two state variables [8]. Moreover, FDM is not

scalable. This is due to the high non-linearity of PDEs governing economic equilibrium models and the computational infeasibility of solving large linear systems when an implicit scheme is employed.

Deep learning, particularly deep neural networks, have been employed for a variety of tasks across multiple domains, including regression, classification, and generation of images and natural language [14]. Recently, the use of deep learning for solving partial differential equations (PDEs) has emerged as a promising alternative to traditional numerical solutions [4, 26]. This approach leverages the theorem that neural networks can serve as universal function approximators [18]. The primary methodology involves Physics-Informed Neural Networks (PINNs), which optimize neural networks using PDEs as loss functions to approximate solutions [31, 30]. However, to the best of our knowledge, deep learning has not been extensively utilized to solve equilibrium problems in continuous time economics, in comparison to the PINN literature.¹ These problems typically involve optimizing Hamilton-Jacobi-Bellman (HJB) equations, which often lack classical smooth solutions [22, 36]. Additionally, they are coupled with a system of algebraic equations derived from the market clearing conditions, binding constraints and financial frictions. Although solving such a system of PDEs can be numerically unstable, neural networks could potentially offer improved approximations.

In this paper, we present Deep-MacroFin, a comprehensive framework for solving PDEs, with a specific focus on continuous time economic models. Compared to traditional numerical methods, our approach offers several advantages: (1) it accommodates higher dimensionality; (2) it handles differentiation more accurately without the need for explicit discretization; (3) it leverages the proven effectiveness of deep learning for function approximation and PDE solution; and (4) once trained and the problem solved, the solution can be extrapolated to a larger domain, free from grid space constraints. Furthermore, our methods outperform existing neural network techniques in several ways: (1) they offer simpler, more user-friendly implementation and usage, with support for string and \LaTeX input; (2) they can readily approximate discontinuous functions within constrained systems; and (3) they allow for flexible initial/boundary conditions, enabling a shift in learning focus and accommodating various boundary shapes in high dimensions.

2 Related Work

While several libraries exist for numerically solving PDEs, they either struggle with high-dimensional problems or gear towards physical rather than economic systems. Deep-MacroFin aims to fill these gaps by providing a comprehensive, user-friendly solution for modeling economic equilibrium with PDEs. We benchmark our approach against two existing libraries for evaluation.

PyMacroFin [9]. This library is dedicated to solve macro-finance equilibrium problems in continuous-time with one or two state variables, following the approach in [7]. It uses the traditional finite difference method with implicit (backward) schemes, assumed to be more stable than forward schemes. Due to the nonlinearity of HJB equations, stability and convergence cannot be guaranteed. Therefore, an auxiliary linear parabolic time-dependent PDE is used to represent the HJB equations, treating them as linear and introducing non-linearity through transient time iterations. However, due to numerical stability issues, PyMacroFin can only solve problems with up to two state variables. For general economic problems in higher dimensions, or even with two state variables, the finite difference method could break down or slow down significantly due to grid size expansion [8].

DeepXDE [26]. This library utilizes PINNs to solve both forward and inverse PDE problems using deep neural networks. It can handle forward problems with given initial and boundary conditions, and inverse problems with provided measurements. DeepXDE has been used to solve the option pricing problem [35], and a dynamic equilibrium problem similar to our formulation [12]. While DeepXDE is suitable for a variety of PDE solving tasks, it does have certain limitations. To solve forward PDE problems effectively, users must explicitly define first and second order derivatives using the provided Jacobian and Hessian functions, and supply initial and boundary conditions, which are typically unknown for equilibrium macro-finance problems. Additionally, in some instances, a reference solution must be provided for the training to proceed correctly, which can limit its applicability.

3 Methodology

3.1 Problem Formulation

We consider two types of agents in our model: households (h) and intermediaries (i), indexed by $j \in \{h, i\}$. These agents differ in their consumption preferences and both possess stochastic differential utility [10]. Time is continuous and its horizon is infinite. There is a risky asset (capital, k_t^p) and riskless bond that the agents can trade freely. The

¹This area is still nascent, albeit growing over time.

evolution of the capital is given by

$$\frac{dk_t^a}{k_t^a} = (\mu^a + \Phi(\iota_t^a))dt + \sigma^a dZ_t^a, \quad (1)$$

where μ^a , σ^a , ι_t^a represent growth rate, volatility and investment function of capital, respectively. $\Phi(\iota_t^a)$ is a functional form for the investment function, and Z_t^a is a standard Brownian motion with filtration \mathcal{F}_t . The probability space is $(\Omega, \mathcal{F}_t, \mathcal{P})$. We assume no transaction costs or frictions, for simplicity. Let the price of capital be denoted as q_t^a . Its dynamics is conjectured as

$$\frac{dq_t^a}{q_t^a} = \mu_t^{qa} dt + \sigma_t^{qa} dZ_t^a \quad (2)$$

Agent j maximizes their lifetime expected utility, subject to their budget constraint. The objective function is given as

$$U_t^j = \sup_{c_t^j, w_t^{ja}, \iota_t^{ja}} \mathbb{E}_t^{\mathcal{P}} \left[\int_t^\infty f(c_s^j, U_s^j) ds \right], \quad (3)$$

where c_t^j denotes agent j 's consumption process, w_t^{ja} represents the portfolio weight indicating agent j 's long/short positions, and ι_t^{ja} is agent j 's investment function. The function $f(c, U)$ is a normalized aggregator of consumption and continuation value in each period. In equilibrium, $\iota_t^{ia} = \iota_t^{ha} = \iota_t^a$. The budget constraint is

$$\frac{dn_t^j}{n_t^j} = \mu_t^{nj} dt + \sigma_t^{nja} dZ_t^a. \quad (4)$$

The agents have Epstein-Zin preferences [11] depending on agent wealth multipliers ξ_t^j . The dynamics of ξ_t^j is

$$\frac{d\xi_t^j}{\xi_t^j} = \mu_t^{\xi j} dt + \sigma^{\xi ja} dZ_t^a \quad (5)$$

The HJB equation to solve for optimality is:

$$0 = \sup_{w_t^{ja}, \iota_t^{ja}, c_t^j} f(c_t^j, U_t^j) + \mathbb{E}_t(dU_t^j), \quad (6)$$

which can be highly non-linear elliptical PDE depending on the problem.

We construct a Markov equilibrium in one state variable: $\eta_t := \frac{n_t^i}{n_t^i + n_t^h}$, which denotes the share of wealth held by agent i . Let $\sigma_t^{na} := \eta_t \sigma_t^{nia} + (1 - \eta_t) \sigma_t^{nha}$. The dynamic of η_t is given by

$$\frac{d\eta_t}{\eta_t} = \mu_t^\eta dt + \sigma_t^{\eta a} dZ_t^a. \quad (7)$$

The market clearing conditions, where the quantity supplied is equal to the quantity demanded at the clearing price, can be formulated as algebraic equations:

$$\mathcal{M}_k(\eta_t, w_t^{ia}, w_t^{ha}, c_t^i, c_t^h, \dots) = 0 \quad (8)$$

In this model, agent wealth multipliers (ξ_t^i, ξ_t^h) and endogenous variables $(\mu_t^\eta, \sigma_t^{\eta a}, q_t^a, w_t^{ia}, w_t^{ha})$ are unknown and expected to be approximated by neural networks. The model is defined on a single state variable, $\eta_t \in [0, 1]$. Learning is guided by the HJB equation defined in (6) and endogenous equations \mathcal{E}_k , parameterized by constant parameters $\lambda = \{\gamma^j, \zeta^j, \rho^j, \dots\}$:

$$\mathcal{E}_k \left(\eta_t; \xi_t^i, q_t^a, \dots; \frac{\partial \xi_t^i}{\partial \eta_t}, \dots; \frac{\partial^2 \xi_t^i}{\partial \eta_t^2}, \dots; \lambda \right) = 0 \quad (9)$$

The endogenous equations encompass market clearing conditions, and optimality conditions for the HJB equations.

This framework can be extended to multiple agents with additional state variables, leading to problems in higher dimensional spaces.

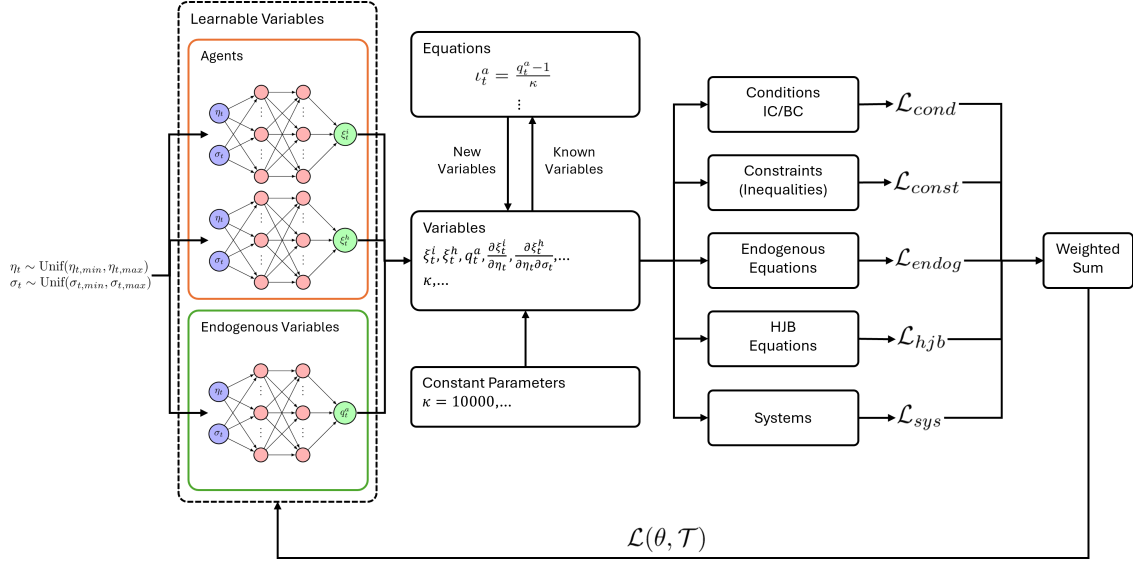


Figure 1: System Overview. The model assumes the presence of two state variables: η_t (wealth share) and σ_t (volatility), two agents: ξ_t^h (households) and ξ_t^i (intermediaries), and one endogenous variable: q_t^a (price of the capital).

3.2 System Overview

As outlined in the previous section, agent wealth multipliers and endogenous variables are approximated by neural networks, guided by endogenous and HJB equations. In a broader context, the model could also be guided by inequality constraints, initial and boundary conditions, and constraint-activated systems, the details of which will be discussed in subsequent sections. Let θ be the neural network parameters, \mathcal{T} be the training data. With some abuse of index notation, the overall loss function is defined as:

$$\begin{aligned} \mathcal{L}(\theta, \mathcal{T}) = & \sum_i \lambda_{cond,i} \mathcal{L}_{cond,i} + \sum_i \lambda_{const,i} \mathcal{L}_{const,i} \\ & + \sum_i \lambda_{endog,i} \mathcal{L}_{endog,i} + \sum_i \lambda_{hjb,i} \mathcal{L}_{hjb,i} \\ & + \sum_i \lambda_{sys,i} \mathcal{L}_{sys,i}, \end{aligned} \quad (10)$$

which is a weighted sum of losses from all conditions, constraints, endogenous equations, HJB equations, and systems, with each loss computation detailed in subsequent sections. This weighted loss guides the neural network to accurately learn the equilibrium solution. There exist strategic ways to optimally select the weights λ_i s to guarantee convergence, such as the use of neural tangent kernels [19] or heuristic adaptation [27]. However, in our current context, we fix $\lambda_i = 1$ for all problems and all loss functions. Models that minimize $\mathcal{L}(\theta, \mathcal{T})$ are expected to encapsulate all necessary information from the provided guidance. Figure 1 provides an overview of the system for a case with two state variables. Each component of the system and the training details will be elaborated in the following sections.

3.3 State Variables

The state variables $X = (x_1, \dots, x_d) \in \mathbb{R}^d$ define the dimensionality of the problem. In physical problems, these variables could represent positions in time and space, while in economic problems, they could denote the proportion of wealth held by a specific agent or the volatility of capital returns. Users can specify a domain $x_i \in [low_i, high_i]$ for each state variable. During training, these variables are independently sampled as $x_i \sim \text{Unif}(low_i, high_i)$. By default, the domain is set to $x_i \in [-1, 1]$, which means the variables are uniformly sampled from the interval $[-1, 1]$.

3.4 Parameters

These are constant hyper-parameters governing the model. In the context of economic models, these could encompass factors such as relative risk aversion (γ), intertemporal elasticity of substitution (ζ), discount rate (ρ), productivity (α), etc. Different parameters can yield different solutions for the same underlying model.

3.5 Learnable Variables

Learnable variables include agent wealth multipliers and endogenous variables. These are the unknown variables to approximate. These variables, which have no specific format restrictions, can represent any unknown functions $f : \mathbb{R}^n \rightarrow \mathbb{R}$ to be learned by neural networks. The learnable variables are implemented as configurable deep neural networks. Number of hidden units and layers, and types of activation functions can be customized. Currently Multi-Layer Perceptrons (MLPs) [14] and Kolmogorov-Arnold Networks (KANs) [24] are supported.

MLP is a fully connected feedforward neural network. This means that all nodes in one layer (input or hidden) are connected to all nodes in the subsequent layer. An MLP consists of at least three layers of nodes: an input layer, a hidden layer, and an output layer. An MLP of L layers is defined by the following:

$$\begin{aligned} f^l(x) &= \sigma^l(W^l x + b^l), 1 \leq l \leq L \\ f(x) &= f^L \circ f^{L-1} \circ \dots \circ f^1(x) \end{aligned}$$

where x is the input value, $W^l \in \mathbb{R}^{o_l \times i_l}$ denotes the weights, i_l is the layer input size, o_l is the layer output size, $b \in \mathbb{R}^{o_l}$ is the bias, and σ^l is an activation function such as hyperbolic tangent (tanh), sigmoid, rectified linear unit ($\text{ReLU}(x) = \max(x, 0)$) or sigmoid linear unit ($\text{SiLU}(x) = x\sigma(x)$). The universal approximation theorem [18] underlies MLP. An n -input MLP with sufficiently many hidden units and non-linear activation can approximate any Borel-measurable function $f : \mathbb{R}^n \rightarrow \mathbb{R}$.

KAN is based on Kolmogorov-Arnold representation theorem, which posits that if $f : [0, 1]^n \rightarrow \mathbb{R}$ is a multivariate continuous function, then f can be expressed as a finite composition of continuous functions of a single variable and the binary operation of addition:

$$f(x) = \sum_{q=1}^{2n+1} \Phi_q \left(\sum_{p=1}^n \phi_{q,p}(x_p) \right), \quad (11)$$

where $\phi_{q,p} : [0, 1] \rightarrow \mathbb{R}$, $\Phi_q : \mathbb{R} \rightarrow \mathbb{R}$. KAN is claimed to outperform MLP in terms of accuracy and interpretability. However, recent research suggests that KAN requires further improvements to match MLP in solving PDEs due to its lack of robustness and computational parallelism [33].

Automatic differentiation facilitates the precise and efficient calculation of derivatives [3, 28]. Following the forward pass, where output values are computed based on input values, a backward pass propagates gradients back to each weight, bias, and input value. This process enables the computation of all differential operators in any PDEs. Unlike PyMacroFin, which supports derivatives up to the second order, or DeepXDE, which necessitates users to employ Jacobian and Hessian for first and second order derivative computations, Deep-MacroFin utilizes a dynamic programming approach for higher order differentiation. The pseudocode is provided in Algorithm 1. This approach allows users to implicitly use derivatives of any degree to define new variables and compute losses. For example, suppose there are two state variables x_1 and x_2 . In the first iteration, lambda functions to compute $f_{x_1}(\frac{\partial f}{\partial x_1})$ and $f_{x_2}(\frac{\partial f}{\partial x_2})$ are constructed using automatic differentiation. Then in the second iteration, lambda functions for $f_{x_1 x_1}(\frac{\partial^2 f}{\partial x_1^2})$ and $f_{x_1 x_2}(\frac{\partial^2 f}{\partial x_1 \partial x_2})$ are computed based on the lambda function to compute f_{x_1} , while those for $f_{x_2 x_1}(\frac{\partial^2 f}{\partial x_1 \partial x_2})$ and $f_{x_2 x_2}(\frac{\partial^2 f}{\partial x_2^2})$ are computed based on f_{x_2} . These derivatives, along with the original function f , are stored in a string-to-function mapping for formula evaluation. Even though $f_{x_1 x_2}$ and $f_{x_2 x_1}$ are identical for continuous functions, both are saved to allow users to input derivatives in any sequence in their formula strings.

3.6 Formula Evaluation

User-provided formulas can be raw Python formula strings or \LaTeX -based formula, which is not supported in Py-MacroFin. The parsing of \LaTeX is based on a regular expression approach, independent of external libraries. This allows users to easily transfer their formulas from \LaTeX documents to Python code.

3.7 Equations

The Equation module is used to define new variables. In economic models, the endogenous or HJB equations guiding the equilibrium are unlikely to directly depend on the agent wealth multipliers and endogenous variables. The Equation module provides a straightforward method to define intermediate variables. Given an equation $l = r(x)$, l is stored as a new variable in the system with an initial value of zero. During each iteration of training and testing, $r(x)$ is evaluated using known variables, and the resulting value is assigned to l . For example, the equation $\iota_t^a = \frac{q_t^a - 1}{\kappa}$ in Figure 1 defines a new variable ι_t^a . Its value is updated to $\frac{q_t^a - 1}{\kappa}$ in each iteration.

Algorithm 1 Derivative Computation

Input: f : the neural network to compute derivatives on,
 X : state variables,
 O : maximum order of derivatives to compute
Output: df : all derivatives of f , up to O order, w.r.t. all variables in X

- 1: Initialize $df_{level} = \{1 : \{\}, 2 : \{\}, \dots, O : \{\}\}$. {Derivatives of each order}
- 2: **for** $x_i \in X$ with name xi **do**
- 3: $df_{level}[1][f_xi] \leftarrow$ lambda expression for first order derivative of f w.r.t. x_i
- 4: **end for**
- 5: **for** $o = 2$ to O **do**
- 6: **for** $x_i \in X$ with name xi **do**
- 7: **for** $f_prev \in df_{level}[o - 1]$ **do**
- 8: $df_{level}[o][f_prevxi] \leftarrow$ lambda expression for first order derivative of f_prev w.r.t. x_i
- 9: **end for**
- 10: **end for**
- 11: **end for**
- 12: Construct $df = \{f_xi : f_{x_i}, \dots\}$ by removing first order keys in df_{level}
- 13: **return** df

3.8 Conditions

Each learnable variable $v_i \in \{a_1, \dots, a_n, e_1, \dots, e_m\}$, either an agent wealth multiplier or an endogenous variable, can be associated with specific conditions $\mathcal{C}(v_i, x) = 0$. In the context of mathematical or physical PDE problems, these conditions could represent initial value conditions $v_i(x_0) = v_{i0}$ or boundary value conditions $\mathcal{B}(v_i, x) = 0$, where $x \in \partial\Omega$, and $\Omega \subset \mathbb{R}^d$ is the problem domain. These conditions could be extended to any points or subsets $U \subset \Omega \cup \partial\Omega$ that require accurate approximation. This information is supplied to the neural network as a Mean Squared Error (MSE) loss over the set U :

$$\mathcal{L}_{cond} = \frac{1}{|U|} \sum_{x \in U} \|\mathcal{C}(v_i, x)\|_2^2. \quad (12)$$

3.9 Endogenous Equations

The Endogenous Equation module is used to establish equalities that are required to pin down endogenous variables in the system. Typically, an endogenous equation takes the form of an algebraic (partial differential) equation $l(x) = r(x)$. Each endogenous equation is converted to a MSE loss over a batch of size B :

$$\mathcal{L}_{endog} = \frac{1}{B} \|l(x) - r(x)\|_2^2. \quad (13)$$

3.10 HJB Equations

The HJB Equation module is used to inform the neural networks of the heterogenous agent asset pricing models. Unlike PyMacroFin, which linearizes the HJB equation, Deep-MacroFin allows for direct input of HJB equations in the form of (6) to pin down each agent. As we aim for the optimal value of the HJB equation $\sup\{\text{HJB}(x)\}$ to be zero, the MSE loss can be computed over a batch of size B as:

$$\mathcal{L}_{hjb} = \frac{1}{B} \|\text{HJB}(x)\|^2 \quad (14)$$

The optimality conditions are computed using first-order conditions and are enforced using equations and endogenous equations.

3.11 Constraints

The Constraint module is used to establish inequalities necessary for constraining the model, primarily used for constraint-activated systems. It could also inform the neural network of inequality constraints when the acceptable solution does not strictly lie on a hyperplane (manifold) defined by an endogenous equation. For $l(x) \leq r(x)$, a rectified MSE is computed over a batch of size B :

$$\mathcal{L}_{const} = \frac{1}{B} \|\text{ReLU}(l(x) - r(x))\|_2^2, \quad (15)$$

Algorithm 2 Training Step

Input: Agents a_1, \dots, a_n , endogenous variables e_1, \dots, e_m , with neural network parameters θ

- 1: Sample a batch (size B , default $B = 100$) of state variables $X = (x_1, \dots, x_d)$, $x_i \sim \text{Unif}(\text{low}_i, \text{high}_i)$
- 2: **for all** $v_i \in \{a_1, \dots, a_n, e_1, \dots, e_m\}$ **do**
- 3: Compute $v_i(\theta, X)$, and all associated derivatives
- 4: **end for**
- 5: **for all** eq \in equations **do**
- 6: Update eq.lhs by evaluating eq.rhs
- 7: **end for**
- 8: Compute losses using conditions, constraints, endogenous equations, HJB equations and systems
- 9: Compute the total loss $\mathcal{L}(\theta, \mathcal{T})$ with (10)
- 10: Backward propagation and update θ to minimize $\mathcal{L}(\theta, \mathcal{T})$

where $\text{ReLU}(x) = \max(x, 0)$. Therefore, loss is only computed for $x \in B$, where $l(x) > r(x)$, *i.e.* when the constraint $l(x) \leq r(x)$ is not satisfied. For $l(x) \geq r(x)$, the rectified MSE is computed as

$$\mathcal{L}_{\text{const}} = \frac{1}{B} \|\text{ReLU}(r(x) - l(x))\|_2^2. \quad (16)$$

In the case of strict inequalities, $l(x) > r(x)$ or $l(x) < r(x)$, an additional $\epsilon = 10^{-8}$ is added to the difference within ReLU to ensure strict inequalities.

3.12 Systems

Systems are activated only when the binding constraints are satisfied. For a batch of inputs, both constraint-governed equations and endogenous equations are computed for each input in the batch. If an input does not satisfy the constraint, it is excluded from the loss computation. Equations are used to assign new variables and losses are computed based on the associated endogenous equations.

Let $\mathbb{1}_{\text{mask}}$ be a vector of zeros and ones indicating which inputs in the batch meet the constraints. Then loss for a specific endogenous equation i in the system is

$$\mathcal{L}_{\text{endog},i} = \frac{1}{\sum \mathbb{1}_{\text{mask}}} \langle (l - r)^2, \mathbb{1}_{\text{mask}} \rangle, \quad (17)$$

where $(l - r)^2$ is the element-wise square of $l - r$, and $\langle \cdot, \cdot \rangle$ denotes the inner product. Essentially, this is the MSE loss computed on mask-selected inputs. Let λ_i be the weight associated with each endogenous equation, and N be the number of endogenous equations attached to the system. The total loss of the system is

$$\mathcal{L}_{\text{sys}} = \sum_{i=1}^N \lambda_i \mathcal{L}_{\text{endog},i}. \quad (18)$$

3.13 Training

If the learnable variables are exclusively defined using MLPs, the neural networks can be trained using L-BFGS [23], Adam [21], and AdamW [25] algorithms. However, if any of the learnable variables are defined using KANs, then the neural networks will be trained using the KAN-customized L-BFGS algorithm [24]. The neural networks are trained for a fixed amount of epochs pre-defined by the users. Random seed is set to zero before training to ensure reproducibility. Within each epoch, the training process outlined in Algorithm 2 is executed. The objective is to approximate the optimal neural network parameters $\theta^* = \arg \min \mathcal{L}(\theta, \mathcal{T})$. Upon completion of the training, both the model with the lowest loss and the model from the final epoch are saved for future use.

3.14 Limitations

Currently, \LaTeX parsing is based on basic regular expression matching. Not all \LaTeX symbols are supported (*e.g.* floor/ceiling functions, which are typically not used in PDE settings.), and some preprocessing is necessary. Due to string execution, GPU acceleration of PyTorch may not enhance computation speed. As such, CPU computation is currently the preferred method.

4 Experiments

To evaluate Deep-MacroFin’s performance, we undertake a variety of tasks: basic ODEs, log utility model, and the 1D economic model outlined in Section 3.1. This section showcases a selection of representative examples. All models are trained on a machine running Windows 11, with an i7-12700H CPU and 16GB RAM. The backend utilizes PyTorch 2.3.0.

4.1 Function Approximation

To validate the basic functionality of function approximation using MLPs, consider the discontinuous oscillating function presented in [33]:

$$y = \begin{cases} 5 + \sum_{k=1}^4 \sin(kx), & x < 0 \\ \cos(10x), & x \geq 0 \end{cases} \quad (19)$$

We adhere to the same setup as in the referenced article. The state variable is $x \in [-3, 3]$. An endogenous variable y is configured as a 2-layer MLP, each layer containing 40 hidden units and activated by SiLU. The model is trained for 50000 epochs using the Adam optimizer with a learning rate of 10^{-3} . The fitted function, along with its first and second order derivatives and the loss convergence, can be observed in Figure 2. The original function is almost perfectly fitted, but the first and second order derivatives exhibit significant deviations around discontinuity. This is a recognized limitation of neural networks in approximating higher order derivatives [37, 32]. DeepXDE converges to a loss around 10^{-4} with algorithmic enhancements. PyMacroFin, which does not support constrained systems on state variables, was not trained.

4.2 Second Order ODE

Consider the Cauchy-Euler equation:

$$x^2 y'' + 6xy' + 4y = 0, y(1) = 6, y(2) = \frac{5}{4}, \quad (20)$$

with solution $y = 4x^{-4} + 2x^{-1}$. In this example, we specifically compare the performance of MLPs and KANs in solving PDEs. A summary of the model configuration and performance is reported in Table 1. The MLP model is trained using the Adam optimizer with a learning rate of 10^{-3} . The same model, when trained using DeepXDE, exhibits a similar loss and training time. On the other hand, the KAN model is trained using the customized L-BFGS optimizer with a learning rate of 1. The computation of KAN heavily relies on activation functions rather than matrix multiplication, and the optimization is performed with a customized L-BFGS. As a result, the computational speed of KAN is significantly slower than that of MLP. However, KAN utilizes far fewer parameters while still achieving a good fit for both the function and its associated derivatives except for the region close to 1, which leads to higher loss. Figure 3 shows the fitted models. The fitting of the first and second order derivatives is accurate. This is due to the fact that the function under consideration is continuously differentiable. Furthermore, the differential equation regulates higher order derivatives.

Type	Hidden	#Params	Epochs	Time	Loss
MLP	[30]*4	2881	2000	13.1s	0.0009
KAN	[5]*2	641	100	79.7s	0.1453

Table 1: MLP and KAN Comparison

4.3 Diffusion Equation

Consider the diffusion equation:

$$\frac{\partial y}{\partial t} = \frac{\partial^2 y}{\partial x^2} - e^{-t}(\sin(\pi x) - \pi^2 \sin(\pi x)), \quad (21)$$

with $x \in [-1, 1]$, $t \in [0, 1]$, $y(x, 0) = \sin(\pi x)$, $y(-1, t) = y(1, t) = 0$. The solution is $y = e^{-t} \sin(\pi x)$. We maintain identical settings for both Deep-MacroFin and DeepXDE: 4-layer MLP with each layer containing 30 hidden units and tanh activation. During each epoch, we sample 100 points within the domain, along with 100 points each for the initial and boundary conditions. Both models undergo training for a total of 1000 epochs, which take 10 second for both frameworks on CPU. Both models converge with final losses on the scale of 10^{-3} . Figure 4 shows the fit achieved by Deep-MacroFin and DeepXDE.

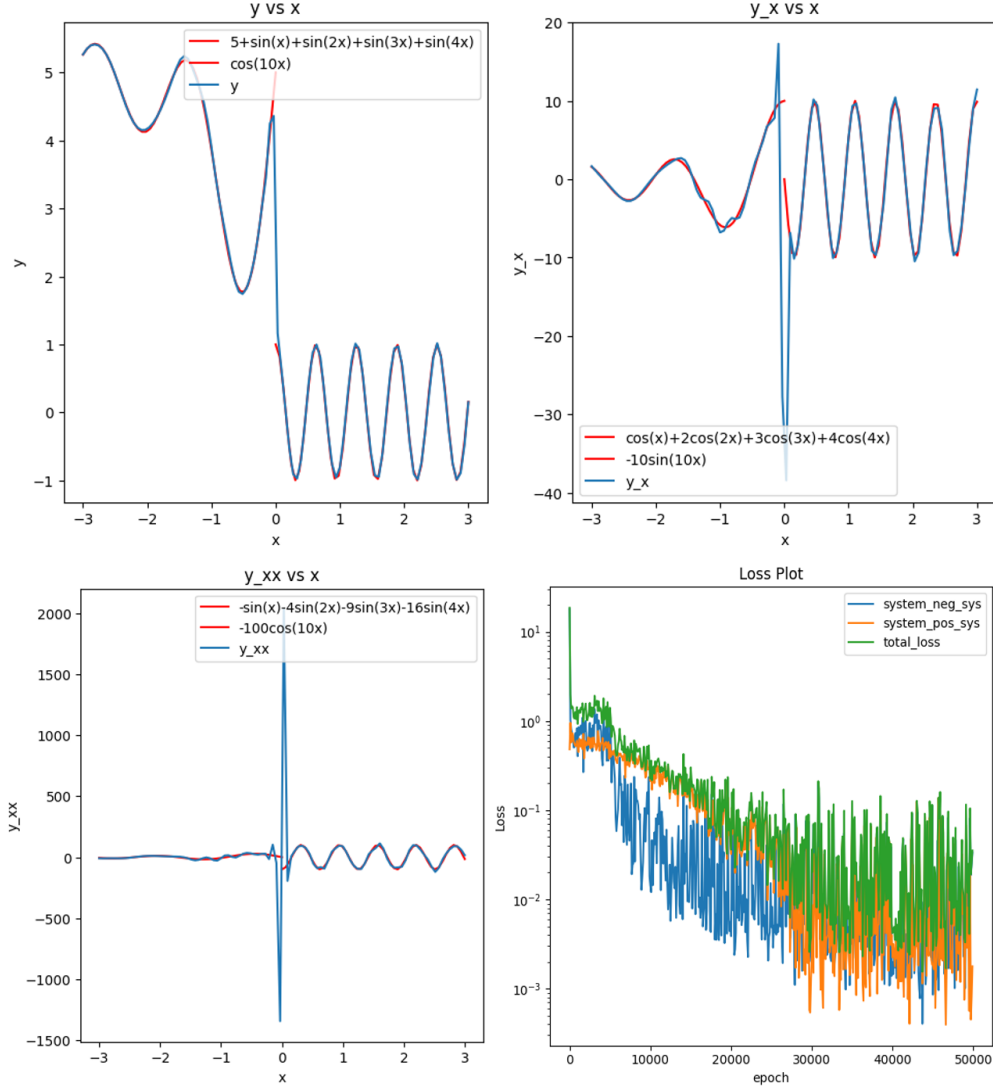


Figure 2: Function Approximation: Red shows the exact function and derivatives; blue shows the fitted models.

4.4 Log Utility

We replicate the log-utility results from Proposition 4 in [7] and benchmark them against the PyMacroFin solution, which starts from an initial guess. The functions q and ψ are approximated using 4-layer MLPs, each containing 30 hidden units and SiLU activation. During training, σ_t^q is defined using $\sigma_t^q = \frac{\sigma}{1 - \frac{1}{q} \frac{\partial q}{\partial \eta} (\psi - \eta)} - \sigma$. We solve for the following system of PDEs when $\psi < 1$:

$$\begin{aligned} (r(1 - \eta) + \rho\eta)q &= \psi a_e + (1 - \psi)a_h - \iota \\ (\sigma + \sigma_t^q)^2 \frac{q(\psi - \eta)}{\eta(1 - \eta)} &= a_e - a_h, \end{aligned}$$

and the following PDE when $\psi = 1$:

$$(r(1 - \eta) + \rho\eta)q = a_e - \iota.$$

Figure 5 shows the fitted models (labelled NN) after 20000 epochs alongside the PyMacroFin solution. The models capture the shape of the exact solution from [7]. η^ψ , after where $\psi(\eta) = 1$, is approximately 0.3, aligning with [7] and PyMacroFin solutions. However, neural networks smooth the discontinuity in first order derivative at η^ψ . For future improvements, active learning could be employed [15]. With active learning, the system would identify the subdomain

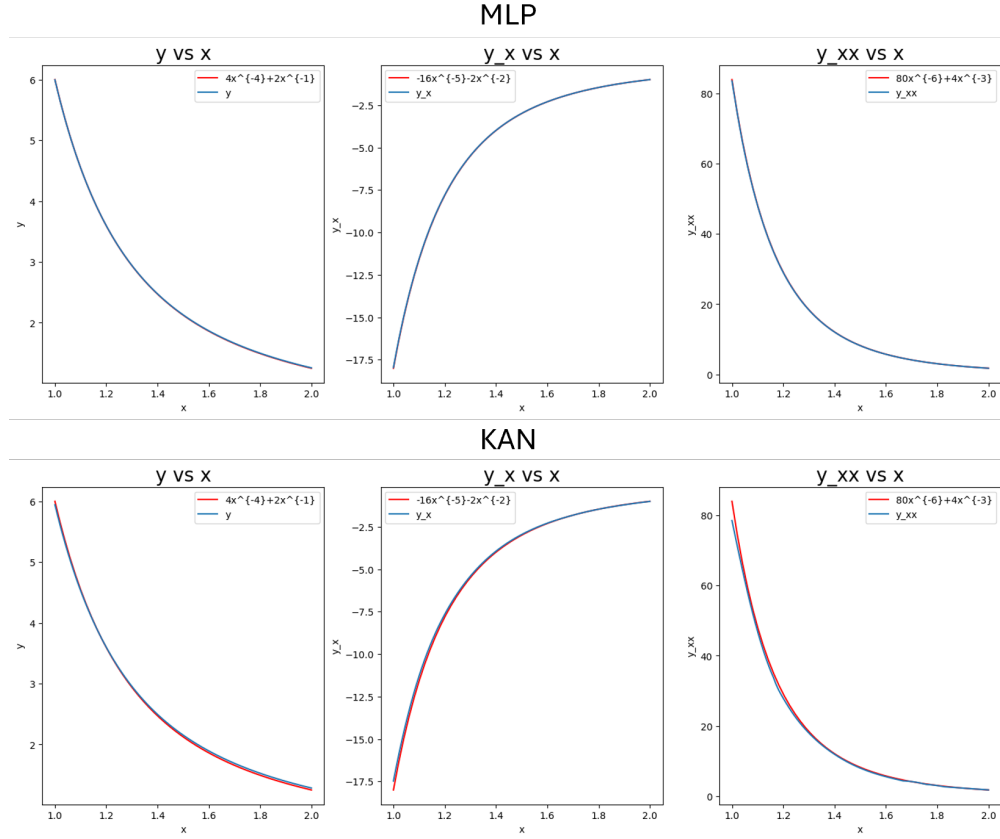


Figure 3: Cauchy-Euler Equation: Exact solution and fitted models by MLP and KAN.

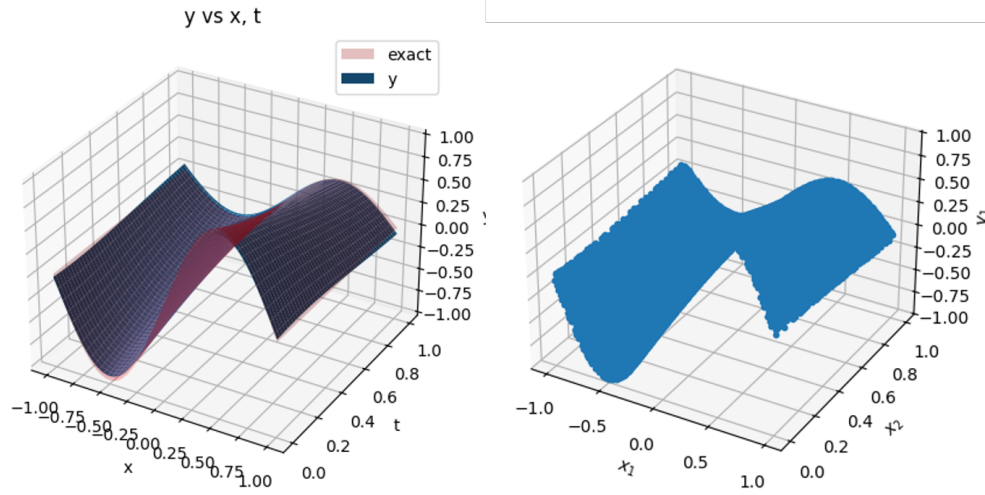


Figure 4: Diffusion Equation: The exact solution and the fitted model by Deep-MacroFin are shown on the left. The fitted model by DeepXDE is shown on the right.

where regime shifts, and actively sample more data points within this specific subdomain to expedite convergence and improve approximation accuracy.

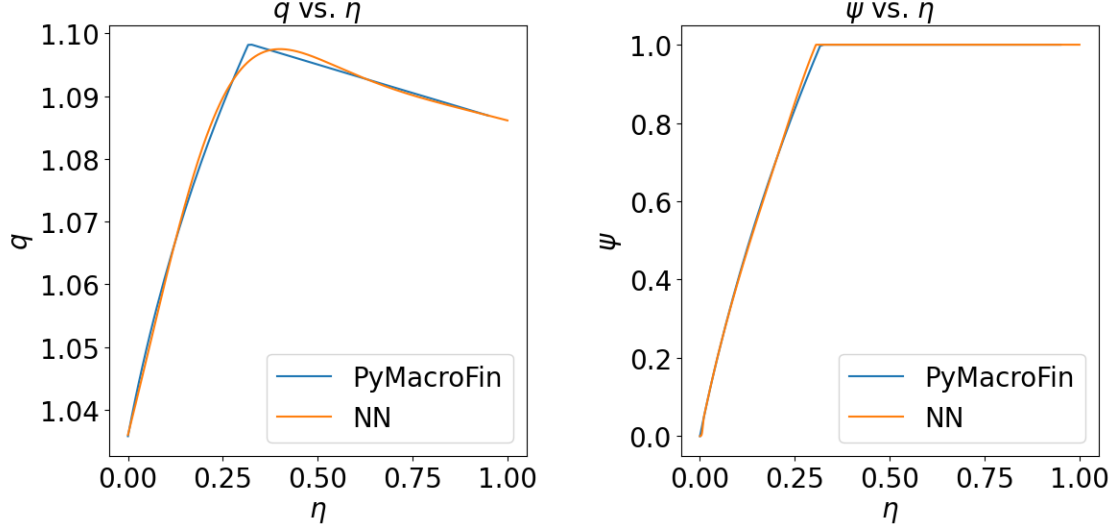


Figure 5: Solutions to the log-utility problem.

4.5 1D Economic Model

The agent wealth multipliers (ξ_t^i, ξ_t^h) and endogenous variables ($\mu_t^\eta, \sigma_t^{\eta^a}, q_t^a, w_t^{ia}, w_t^{ha}$), characterized in Section 3.1, are configured as 4-layer MLPs with 30 hidden units per layer and tanh activation. ξ_t^i, ξ_t^h , and q_t^a are constrained by SoftPlus (a smooth approximation to the ReLU function) to ensure positive outputs, thereby guaranteeing that the price of capital and agent wealth remain non-negative. The state variable η_t is restricted to $[0.01, 0.99]$ to avoid instabilities at extreme share holdings. The system is trained for 2000 epochs using Adam optimizer with a learning rate of 10^{-3} , under the endogenous and HJB constraints. Figure 6 presents the approximated functions $q_t^a, \sigma_t^{q^a}, w_t^{ia}$, and w_t^{ha} for parameters $\gamma^i = 2, \gamma^h = 5, \rho^i = \rho^h = 5\%, \zeta^i = \zeta^h = 1.00005, \mu^a = 0.04, \sigma^a = 0.2$ and $\alpha^a = 0.1$. The sentiment factor μ^O is set to 0.04 to equalize the expected returns on capital (r_t^{ka}) and the risk-free bond (r_t) for both agents. κ is set to 10000 to minimize investments. As the share of wealth held by agent i (η_t) increases, so does the price of capital q_t^a . The volatility of the price, represented by $\sigma_t^{q^a}$, peaks when η_t is around $0.3 \sim 0.4$, reflecting the highest uncertainty. At extreme points, $\eta_t \rightarrow 0$ or $\eta_t \rightarrow 1$, $\sigma_t^{q^a} \rightarrow 0$, indicating minimal price uncertainty when one type of agent holds all the wealth. Both agents maintain a long position, as evidenced by the positive portfolio weights w_t^{ia} and w_t^{ha} . When $\eta_t \sim 0$, only agent h is contributing to the total capital, resulting in $w_t^{ha}(0) = 1$. As η_t increases, both weights decrease, with w_t^{ia} decreasing more rapidly (from 2 to 1) than w_t^{ha} (from 1 to 0.3). This ensures the market clearing condition, where the weighted sum of the capital portfolio held by intermediary i and household h always equals the total capital k_t^a .

5 Conclusion

In this paper, we propose Deep-MacroFin, a comprehensive framework to solve continuous time economic models using deep learning techniques. This framework can be seamlessly adapted for tasks such as solving elementary differential equations, and handling systems of differential equations. When compared to existing libraries, Deep-MacroFin stands out due to its fewer restrictions and enhanced user-friendliness. Looking ahead, our future research will encompass more diverse economic models in higher dimensions and models that encapsulate temporal dynamics, moving beyond a sole focus on equilibrium solutions. Additionally, we plan to integrate active learning and loss weight optimization to ensure superior convergence.

Acknowledgement

We thank University of Toronto Data Sciences Institute (DSI) for funding this project.

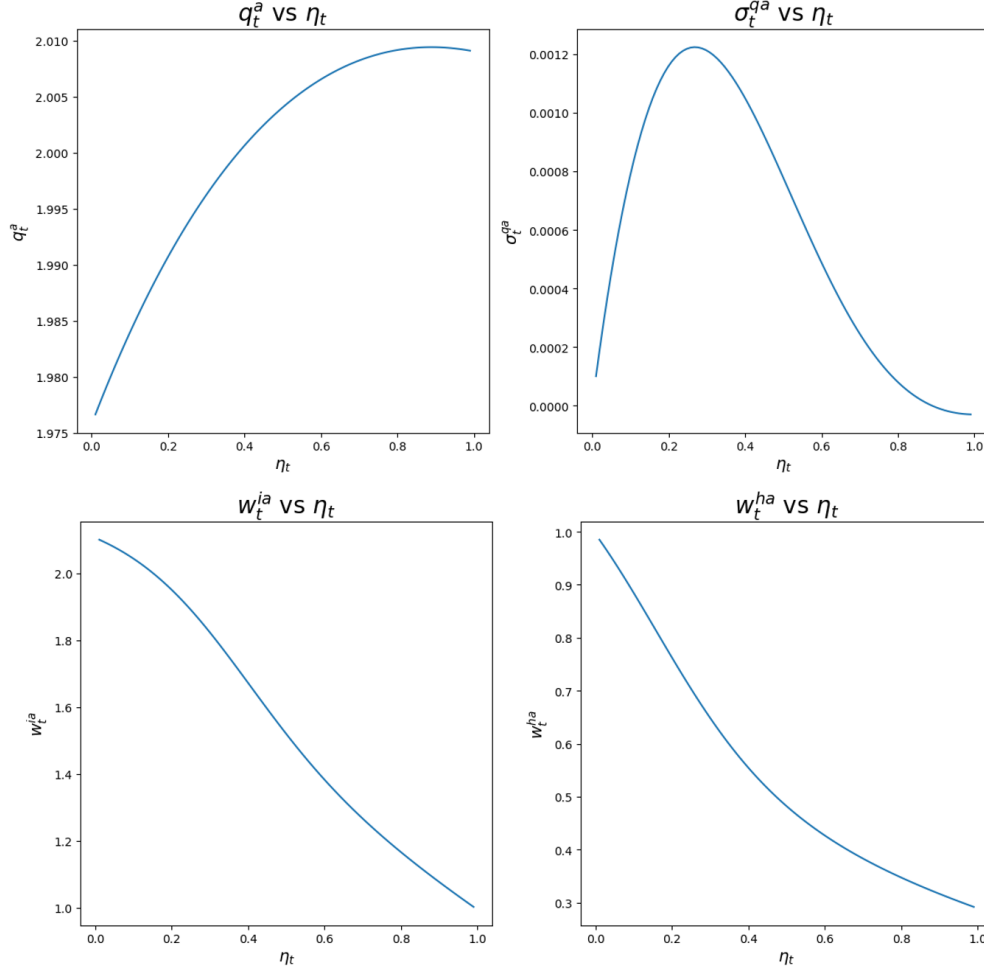


Figure 6: Solutions to the 1D economic problem.

References

- [1] Yves Achdou et al. *Income and Wealth Distribution in Macroeconomics: A Continuous-Time Approach*. Working Paper 23732. National Bureau of Economic Research, Aug. 2017. DOI: 10 . 3386 / w23732. URL: <http://www.nber.org/papers/w23732>.
- [2] Ferri M. H. Aliabadi. “Boundary Element Methods”. In: *Encyclopedia of Continuum Mechanics*. Springer, 2020, pp. 182–193.
- [3] Jason Ansel et al. “PyTorch 2: Faster Machine Learning Through Dynamic Python Bytecode Transformation and Graph Compilation”. In: *29th ACM International Conference on Architectural Support for Programming Languages and Operating Systems, Volume 2 (ASPLOS ’24)*. ACM, Apr. 2024. DOI: 10 . 1145 / 3620665 . 3640366. URL: <https://pytorch.org/assets/pytorch2-2.pdf>.
- [4] Nathan Baker et al. *Workshop Report on Basic Research Needs for Scientific Machine Learning: Core Technologies for Artificial Intelligence*. Tech. rep. USDOE Office of Science, Feb. 2019. DOI: 10 . 2172 / 1478744. URL: <https://www.osti.gov/biblio/1478744>.
- [5] W.E. Boyce and R.C. DiPrima. *Elementary Differential Equations and Boundary Value Problems*. Wiley, 2012. ISBN: 9781118157381. URL: https://books.google.ca/books?id=vf_qMgEACAAJ.
- [6] Markus K Brunnermeier and Yuliy Sannikov. *Macro, Money and Finance: A Continuous Time Approach*. Working Paper 22343. National Bureau of Economic Research, June 2016. DOI: 10 . 3386 / w22343. URL: <http://www.nber.org/papers/w22343>.

- [7] Markus K. Brunnermeier and Yuliy Sannikov. “A Macroeconomic Model with a Financial Sector”. In: *American Economic Review* 104.2 (Feb. 2014), pp. 379–421. DOI: 10.1257/aer.104.2.379. URL: <https://www.aeaweb.org/articles?id=10.1257/aer.104.2.379>.
- [8] Adrien d’Avernas, Damon Petersen, and Quentin Vandeweyer. *A Solution Method for Continuous-Time General Equilibrium Models*. Nov. 18, 2021. URL: <http://www.adriendavernas.com/papers/solutionmethod.pdf>.
- [9] Adrien d’Avernas, Damon Petersen, and Quentin Vandeweyer. *Macro-financial Modeling in Python: PyMacroFin*. Version 0.0.1. Nov. 18, 2021. URL: <https://adriendavernas.com/pymacrofin/index.html>.
- [10] Darrell Duffie and Larry G. Epstein. “Stochastic differential utility”. In: *Econometrica* 60 (1992), pp. 353–394. URL: <https://api.semanticscholar.org/CorpusID:51787219>.
- [11] Larry G. Epstein and Stanley E. Zin. “Substitution, Risk Aversion, and the Temporal Behavior of Consumption and Asset Returns: A Theoretical Framework”. In: *Econometrica* 57.4 (1989), pp. 937–969. ISSN: 00129682, 14680262. URL: <http://www.jstor.org/stable/1913778> (visited on 06/30/2024).
- [12] Benjamin Fan et al. “Deep Learning for Solving and Estimating Dynamic Macro-Finance Models”. In: *arXiv preprint arXiv:2305.09783* (2023). arXiv: 2305.09783 [q-fin.CP]. URL: <https://arxiv.org/abs/2305.09783>.
- [13] Matthieu Gomez. *Asset Prices and Wealth Inequality*. 2017 Meeting Papers 1155. Society for Economic Dynamics, 2017. URL: <https://EconPapers.repec.org/RePEc:red:sed017:1155>.
- [14] Ian Goodfellow, Yoshua Bengio, and Aaron Courville. *Deep Learning*. MIT Press, 2016. URL: <http://www.deeplearningbook.org>.
- [15] Goutham Gopalakrishna. *ALIENs and Continuous Time Economies*. Swiss Finance Institute Research Paper Series 21-34. Swiss Finance Institute, 2021. URL: <https://EconPapers.repec.org/RePEc:chf:rpseri:rp2134>.
- [16] Christian Grossmann, Hans-G. Roos, and Martin Stynes. *Numerical Treatment of Partial Differential Equations*. Springer Science & Business Media, 2007.
- [17] J. Douglas Hoffman and Steven P. Frankel. *Numerical methods for engineers and scientists*. CRC Press, 2001.
- [18] Kurt Hornik, Maxwell Stinchcombe, and Halbert White. “Multilayer feedforward networks are universal approximators”. In: *Neural Networks* 2.5 (1989), pp. 359–366. ISSN: 0893-6080. DOI: [https://doi.org/10.1016/0893-6080\(89\)90020-8](https://doi.org/10.1016/0893-6080(89)90020-8). URL: <https://www.sciencedirect.com/science/article/pii/0893608089900208>.
- [19] Arthur Jacot, Franck Gabriel, and Clément Hongler. “Neural tangent kernel: convergence and generalization in neural networks”. In: *Proceedings of the 32nd International Conference on Neural Information Processing Systems*. NIPS’18. Montréal, Canada: Curran Associates Inc., 2018, pp. 8580–8589.
- [20] Yogesh Jaluria and Satya N. Atluri. “Computational heat transfer”. In: *Computational Mechanics* 14.5 (1994), pp. 385–386.
- [21] Diederik P. Kingma and Jimmy Ba. “Adam: A Method for Stochastic Optimization”. In: *ArXiv abs/1412.6980* (2017). arXiv: 1412.6980 [cs.LG].
- [22] Donald E. Kirk. *Optimal Control Theory: An Introduction*. Courier Corporation, 1970.
- [23] D. C. Liu and J. Nocedal. “On the Limited Memory Method for Large Scale Optimization”. In: *Mathematical Programming B* 45.3 (1989), pp. 503–528.
- [24] Ziming Liu et al. “KAN: Kolmogorov-Arnold Networks”. In: *arXiv preprint arXiv:2404.19756* (2024).
- [25] Ilya Loshchilov and Frank Hutter. “Decoupled Weight Decay Regularization”. In: *ArXiv abs/1711.05101* (2019). arXiv: 1711.05101 [cs.LG].
- [26] Lu Lu et al. “DeepXDE: A Deep Learning Library for Solving Differential Equations”. In: *SIAM Review* 63.1 (2021), pp. 208–228. DOI: 10.1137/19M1274067. eprint: <https://doi.org/10.1137/19M1274067>. URL: <https://doi.org/10.1137/19M1274067>.
- [27] Remco van der Meer, Cornelis Oosterlee, and Anastasia Borovykh. “Optimally weighted loss functions for solving PDEs with Neural Networks”. In: *arXiv preprint arXiv:2002.06269* (2021). arXiv: 2002.06269 [math.NA]. URL: <https://arxiv.org/abs/2002.06269>.
- [28] Adam Paszke et al. “Automatic differentiation in PyTorch”. In: *NIPS-W*. 2017.
- [29] Alfio Quarteroni and Alberto Valli. *Numerical Approximation of Partial Differential Equations*. Vol. 23. Springer Science & Business Media, 2008.
- [30] Maziar Raissi, Paris Perdikaris, and George E Karniadakis. “Physics-informed neural networks: A deep learning framework for solving forward and inverse problems involving nonlinear partial differential equations”. In: *Journal of Computational Physics* 378 (2019), pp. 686–707.

- [31] Maziar Raissi, Paris Perdikaris, and George Em Karniadakis. “Physics Informed Deep Learning (Part I): Data-driven Solutions of Nonlinear Partial Differential Equations”. In: *arXiv preprint arXiv:1711.10561* (2017).
- [32] Siyuan Shen et al. “HoD-Net: High-Order Differentiable Deep Neural Networks and Applications”. In: *Proceedings of the AAAI Conference on Artificial Intelligence* 36.8 (2022), pp. 8249–8258. DOI: 10.1609/aaai.v36i8.20799. URL: <https://ojs.aaai.org/index.php/AAAI/article/view/20799>.
- [33] Khemraj Shukla et al. “A comprehensive and FAIR comparison between MLP and KAN representations for differential equations and operator networks”. In: *arXiv preprint arXiv:2406.02917* (2024). arXiv: 2406.02917 [cs.LG]. URL: <https://arxiv.org/abs/2406.02917>.
- [34] Pavel Šolín. *Partial Differential Equations and the Finite Element Method*. John Wiley & Sons, 2005.
- [35] X. Wang, J. Li, and J. Li. “A Deep Learning Based Numerical PDE Method for Option Pricing”. In: *Computational Economics* 62 (2023), pp. 149–164. DOI: <https://doi.org/10.1007/s10614-022-10279-x>.
- [36] Jiongmin Yong and Xun Yu Zhou. *Stochastic Controls: Hamiltonian Systems and HJB Equations*. Springer, 1999.
- [37] Quanhui Zhu and Jiang Yang. “A Local Deep Learning Method for Solving High Order Partial Differential Equations”. In: *arXiv preprint arXiv:2103.08915* (2021). arXiv: 2103.08915 [math.NA]. URL: <https://arxiv.org/abs/2103.08915>.

A 1D Economic Model

This appendix provides the mathematical details for the derivation of equations and endogenous equations of the specific model we solve for in Section 3.1. Let $j \in \{h, i\}$ index two types of agents, where h represents households and i represents intermediaries.

A.1 Ito's Lemma Derivations

Given the dynamics of k_t^a (capital), q_t^a (price of capital), ξ_t^j (agent actions) and state variable η_t :

$$\frac{dk_t^a}{k_t^a} = (\mu^a + \Phi(\iota_t^a))dt + \sigma^a dZ_t^a \quad (22)$$

$$\frac{dq_t^a}{q_t^a} = \mu_t^{qa} dt + \sigma_t^{qa} dZ_t^a, \quad (23)$$

$$\frac{d\xi_t^j}{\xi_t^j} = \mu_t^{\xi j} dt + \sigma_t^{\xi ja} dZ_t^a, \quad (24)$$

$$\frac{d\eta_t}{\eta_t} = \left(\underbrace{(1 - \eta_t)(\mu_t^{ni} - \mu_t^{nh}) + (\sigma_t^{na})^2 - \sigma_t^{nia}\sigma_t^{na}}_{\mu_t^\eta} \right) dt + \underbrace{(1 - \eta_t)(\sigma_t^{nia} - \sigma_t^{nha})}_{\sigma_t^{\eta a}} dZ_t^a, \quad (25)$$

where Z_t^a is a standard Brownian motion with filtration \mathcal{F}_t . The probability space is $(\Omega, \mathcal{F}_t, \mathbb{P})$. dZ_t^a is a Wiener process (with $\mu = 0, \sigma = 1$), $(dZ_t^a)^2 = dt$. ι_t^a is investment function of capital, and $\Phi(\iota_t^a)$ is a functional form for the investment function.

Rewrite the process of η_t as $d\eta_t = \mu_t^\eta \eta_t dt + \sigma_t^{\eta a} \eta_t dZ_t^a$. Then

$$\begin{aligned} (d\eta_t)^2 &= (\mu_t^\eta \eta_t dt + \sigma_t^{\eta a} \eta_t dZ_t^a)^2 \\ &= (\sigma_t^{\eta a} \eta_t)^2 dt + (\mu_t^\eta \eta_t)^2 (dt)^2 + 2(\mu_t^\eta \eta_t)(\sigma_t^{\eta a} \eta_t) dt dZ_t^a \\ &= (\sigma_t^{\eta a} \eta_t)^2 dt + o(dt), \end{aligned}$$

where $o(dt) = \{f : |f(\eta_t, t)| < \epsilon|dt|, \forall \epsilon > 0\}$.

Note that the price is a process dependent of the state variable η_t , $q_t^a = q_t^a(\eta_t)$. By Ito's Lemma,

$$\begin{aligned} d(q_t^a(\eta_t)) &= \frac{\partial q_t^a}{\partial \eta_t} d\eta_t + \frac{1}{2} \frac{\partial^2 q_t^a}{\partial \eta_t^2} (d\eta_t)^2 \\ &= \frac{\partial q_t^a}{\partial \eta_t} (\mu_t^\eta \eta_t dt + \sigma_t^{\eta a} \eta_t dZ_t^a) + \frac{1}{2} \frac{\partial^2 q_t^a}{\partial \eta_t^2} (\sigma_t^{\eta a} \eta_t)^2 dt \\ &= \left(\frac{\partial q_t^a}{\partial \eta_t} \mu_t^\eta \eta_t + \frac{1}{2} \frac{\partial^2 q_t^a}{\partial \eta_t^2} (\sigma_t^{\eta a} \eta_t)^2 \right) dt + \frac{\partial q_t^a}{\partial \eta_t} \sigma_t^{\eta a} \eta_t dZ_t^a \end{aligned}$$

Now match the terms with $\frac{dq_t^a}{q_t^a} = \mu_t^{qa} dt + \sigma_t^{qa} dZ_t^a$,

$$\begin{aligned} \mu_t^{qa} &= \frac{1}{q_t^a} \left(\frac{\partial q_t^a}{\partial \eta_t} \mu_t^\eta \eta_t + \frac{1}{2} \frac{\partial^2 q_t^a}{\partial \eta_t^2} (\sigma_t^{\eta a} \eta_t)^2 \right), \\ \sigma_t^{qa} &= \frac{1}{q_t^a} \frac{\partial q_t^a}{\partial \eta_t} \sigma_t^{\eta a} \eta_t. \end{aligned}$$

Similarly, ξ_t^j is a process dependent of η_t , $\xi_t^j = \xi_t^j(\eta_t)$. Matching terms with $\frac{d\xi_t^j}{\xi_t^j} = \mu_t^{\xi j} dt + \sigma_t^{\xi ja} dZ_t^a$,

$$\begin{aligned} \mu_t^{\xi j} &= \frac{1}{\xi_t^j} \left(\frac{\partial \xi_t^j}{\partial \eta_t} \mu_t^\eta \eta_t + \frac{1}{2} \frac{\partial^2 \xi_t^j}{\partial \eta_t^2} (\sigma_t^{\eta a} \eta_t)^2 \right), \\ \sigma_t^{\xi ja} &= \frac{1}{\xi_t^j} \frac{\partial \xi_t^j}{\partial \eta_t} \sigma_t^{\eta a} \eta_t. \end{aligned}$$

Using Ito's product rule, the process of the value of the capital $q_t^a k_t^a$ is

$$\begin{aligned} d(q_t^a k_t^a) &= q_t^a dk_t^a + k_t^a dq_t^a + dq_t^a dk_t^a, \\ \text{or } \frac{d(q_t^a k_t^a)}{q_t^a k_t^a} &= \frac{dk_t^a}{k_t^a} + \frac{dq_t^a}{q_t^a} + \frac{dq_t^a}{q_t^a} \frac{dk_t^a}{k_t^a} \\ &= (\mu^a + \Phi(\iota_t^a))dt + \sigma^a dZ_t^a + \mu_t^{qa} dt + \sigma_t^{qa} dZ_t^a + \sigma^a \sigma_t^{qa} dt + o(dZ_t^a) \\ &= (\mu^a + \Phi(\iota_t^a) + \mu_t^{qa} + \sigma^a \sigma_t^{qa})dt + (\sigma^a + \sigma_t^{qa})dZ_t^a, \end{aligned}$$

which is the capital gain rate.

Let α^a be the productivity rate. The dividend yield generated by the capital is $(\alpha^a - \iota_t^a)/q_t^a$. The return process is computed as

$$\begin{aligned} dr_t^{ka} &= \text{divident yield} + \text{capital gain rate} \\ &= \left(\underbrace{\mu^a + \Phi(\iota_t^a) + \mu_t^{qa} + \sigma^a \sigma_t^{qa} + \frac{\alpha^a - \iota_t^a}{q_t^a}}_{r_t^{ka}} \right) dt + (\sigma^a + \sigma_t^{qa})dZ_t^a. \end{aligned} \quad (26)$$

A.2 HJB Equation Optimality

Consider the following HJB equation:

$$\begin{aligned} 0 &= \sup_{w_t^{ja}, \iota_t^{ja}, c_t^j} f(c_t^j, U_t^j) + \mathbb{E}_t(dU_t^j) \\ &= \sup_{w_t^{ja}, \iota_t^{ja}, c_t^j} \left\{ \frac{f(c_t^j n_t^j, V_t^j)}{(\xi_t^j n_t^j)^{(1-\gamma^j)}} + \mu_t^{\xi j} + \mu_t^{nj} - \frac{\gamma^j}{2} (\sigma_t^{nja})^2 - \frac{\gamma^j}{2} (\sigma_t^{\xi ja})^2 + (1 - \gamma^j) \sigma_t^{\xi ja} \sigma_t^{nja} \right\}, \end{aligned} \quad (27)$$

where

$$f(c_t^j n_t^j, V_t^j) = \left(\frac{1 - \gamma^j}{1 - 1/\zeta^j} \right) \rho^j V_t^j \left[\left(\frac{c_t^j n_t^j}{[(1 - \gamma^j) V_t^j]^{1/(1-\gamma^j)}} \right)^{1-1/\zeta^j} - 1 \right]. \quad (28)$$

The agents have Epstein-Zin preferences [3]. The value function can be verified as

$$V_t^j = \frac{(n_t^j \xi_t^j)^{1-\gamma^j}}{1 - \gamma^j}. \quad (29)$$

Then, the HJB equation can be rewritten as

$$\begin{aligned} &\frac{f(c_t^j n_t^j, V_t^j)}{(\xi_t^j n_t^j)^{(1-\gamma^j)}} + \mu_t^{\xi j} + \mu_t^{nj} - \frac{\gamma^j}{2} (\sigma_t^{nja})^2 - \frac{\gamma^j}{2} (\sigma_t^{\xi ja})^2 + (1 - \gamma^j) \sigma_t^{\xi ja} \sigma_t^{nja} \\ &= \frac{\rho^j}{1 - 1/\zeta^j} \left[\left(\frac{c_t^j}{\xi_t^j} \right)^{1-1/\zeta^j} - 1 \right] + \mu_t^{\xi j} + \mu_t^{nj} - \frac{\gamma^j}{2} (\sigma_t^{nja})^2 - \frac{\gamma^j}{2} (\sigma_t^{\xi ja})^2 + (1 - \gamma^j) \sigma_t^{\xi ja} \sigma_t^{nja}. \end{aligned}$$

Note that $\mu_t^{nj} = r_t - c_t^j + w_t^{ja}(r_t^{ka} - r_t)$ and $\sigma_t^{nja} = w_t^{ja}(\sigma^a + \sigma_t^{qa})$ from the budget constraint:

$$\frac{dn_t^j}{n_t^j} = \left(\underbrace{r_t - c_t^j + w_t^{ja}(r_t^{ka} - r_t)}_{\mu_t^{nj}} \right) dt + \underbrace{w_t^{ja}(\sigma^a + \sigma_t^{qa})}_{\sigma_t^{nja}} dZ_t^a. \quad (30)$$

Then we get the HJB equation:

$$\begin{aligned}
F(w_t^{ja}, \iota_t^{ja}, c_t^j) &= \frac{\rho^j}{1-1/\zeta^j} \left[\left(\frac{c_t^j}{\xi_t^j} \right)^{1-1/\zeta^j} - 1 \right] + \mu_t^{\xi j} + r_t - c_t^j + w_t^{ja}(r_t^{ka} - r_t) \\
&\quad - \frac{\gamma^j}{2}(w_t^{ja})^2(\sigma^a + \sigma_t^{qa})^2 - \frac{\gamma^j}{2}(\sigma_t^{\xi ja})^2 + (1-\gamma^j)\sigma_t^{\xi ja}w_t^{ja}(\sigma^a + \sigma_t^{qa}) \\
&= \frac{\rho^j}{1-1/\zeta^j} \left[\left(\frac{c_t^j}{\xi_t^j} \right)^{1-1/\zeta^j} - 1 \right] + \mu_t^{\xi j} + r_t - c_t^j \\
&\quad + w_t^{ja} \left(\mu_t^{qa} + \mu^a + \Phi(\iota_t^a) + \sigma^a \sigma_t^{qa} + \frac{\alpha^a - \iota_t^a}{q_t^a} - r_t \right) \\
&\quad - \frac{\gamma^j}{2}(w_t^{ja})^2(\sigma^a + \sigma_t^{qa})^2 - \frac{\gamma^j}{2}(\sigma_t^{\xi ja})^2 + (1-\gamma^j)\sigma_t^{\xi ja}w_t^{ja}(\sigma^a + \sigma_t^{qa})
\end{aligned}$$

Apply KKT to unconstrained $F(w_t^{ja}, \iota_t^{ja}, c_t^j)$, we want $\nabla F(w_t^{ja}, \iota_t^{ja}, c_t^j) = \left(\frac{\partial F}{\partial w_t^{ja}}, \frac{\partial F}{\partial \iota_t^{ja}}, \frac{\partial F}{\partial c_t^j} \right)^T = 0$. This gives the necessary condition for optimality as:

$$\begin{aligned}
\frac{\partial F}{\partial w_t^{ja}} &= (r_t^{ka} - r_t) - \gamma^j w_t^{ja}(\sigma^a + \sigma_t^{qa})^2 + (1-\gamma^j)\sigma_t^{\xi ja}(\sigma^a + \sigma_t^{qa}) = 0; \\
\frac{\partial F}{\partial \iota_t^{ja}} &= w_t^{ja} \left(\Phi'(\iota_t^a) - \frac{1}{q_t^a} \right) = 0; \\
\frac{\partial F}{\partial c_t^j} &= \frac{\rho^j}{1-1/\zeta^j} \frac{1}{(\xi_t^j)^{1-1/\zeta^j}} (1-1/\zeta^j)(c_t^j)^{-1/\zeta^j} - 1 = 0.
\end{aligned}$$

$\frac{\partial F}{\partial w_t^{ja}} = 0$ gives

$$(r_t^{ka} - r_t) - \gamma^j w_t^{ja}(\sigma^a + \sigma_t^{qa})^2 + (1-\gamma^j)\sigma_t^{\xi ja}(\sigma^a + \sigma_t^{qa}) = 0. \quad (31)$$

$\frac{\partial F}{\partial \iota_t^{ja}} = 0$ while $w_t^{ja} \neq 0$ gives

$$\Phi'(\iota_t^a) - \frac{1}{q_t^a} = 0. \quad (32)$$

$\frac{\partial F}{\partial c_t^j} = 0$ with $\zeta^j \approx 1$ gives

$$\begin{aligned}
\rho^j (c_t^j)^{-1} - 1 &\approx 0, \\
c_t^j &\approx \rho^j.
\end{aligned} \quad (33)$$

We take the investment function as

$$\iota_t^a = \frac{q_t^a - 1}{\kappa}. \quad (34)$$

Then the functional form

$$\Phi(\iota_t^a) = \frac{1}{\kappa} \log(1 + \kappa \iota_t^a) \quad (35)$$

We use agent h to compute r_t ,

$$r_t = r_t^{ka} - \gamma^h w_t^{ha}(\sigma^a + \sigma_t^{qa})^2 + (1-\gamma^h)\sigma_t^{\xi ha}(\sigma^a + \sigma_t^{qa}). \quad (36)$$

Then add sentiment to agent i ,

$$r_t^{\hat{ka}} = r_t^{ka} + \frac{\mu^O - \mu^a}{\sigma^a}(\sigma^a + \sigma_t^{qa}). \quad (37)$$

It should satisfy the endogenous equation:

$$r_t^{\hat{ka}} - r_t = \gamma^i w_t^{ia}(\sigma^a + \sigma_t^{qa})^2 - (1-\gamma^i)\sigma_t^{\xi ia}(\sigma^a + \sigma_t^{qa}). \quad (38)$$

A.3 Market Clearing Conditions

Consider the capital for each agent k_t^h and k_t^i , their sum should equal the total capital $k_t^h + k_t^i = k_t^a$. Also recall that $\eta_t = \frac{n_t^i}{n_t^h + n_t^i}$. Total budget should equal total capital gain, so $n_t^h + n_t^i = q_t^a k_t^a$. Then

$$\eta_t = \frac{n_t^i}{n_t^h + n_t^i} = \frac{n_t^i}{q_t^a k_t^a}. \quad (39)$$

When market clears, quantity supplied is equal to the quantity demanded at the clearing price, and consumption from both types of agents equals surplus from the production.

$$\begin{aligned} c_t^i n_t^i + c_t^h n_t^h &= (\alpha^a - \iota_t^a)(k_t^i + k_t^h) \\ c_t^i n_t^i + c_t^h n_t^h &= (\alpha^a - \iota_t^a)k_t^a \\ \frac{c_t^i n_t^i}{q_t^a k_t^a} + \frac{c_t^h n_t^h}{q_t^a k_t^a} &= \frac{\alpha^a - \iota_t^a}{q_t^a} \\ c_t^i \eta_t + c_t^h (1 - \eta_t) &= \frac{\alpha^a - \iota_t^a}{q_t^a} \end{aligned}$$

Now consider the portfolio weights $w_t^{ja} = \frac{k_t^j q_t^a}{n_t^j}$.

$$\begin{aligned} k_t^i + k_t^h &= k_t^a \\ \frac{k_t^i}{k_t^a} + \frac{k_t^h}{k_t^a} &= 1 \\ \frac{k_t^i n_t^i q_t^a}{n_t^i q_t^a k_t^a} + \frac{k_t^h n_t^h q_t^a}{n_t^h q_t^a k_t^a} &= 1 \\ \frac{k_t^i q_t^a}{n_t^i} \eta_t + \frac{k_t^h q_t^a}{n_t^h} (1 - \eta_t) &= 1 \\ w_t^{ia} \eta_t + w_t^{ha} (1 - \eta_t) &= 1 \end{aligned}$$

Therefore, from market clearing conditions, we get two endogenous equations:

$$\alpha^a - \iota_t^a = (c_t^i \eta_t + c_t^h (1 - \eta_t)) q_t^a \quad (40)$$

$$1 = w_t^{ia} \eta_t + w_t^{ha} (1 - \eta_t) \quad (41)$$

A.4 Model Details

The definition of constant parameters are provided in Table 2 and the definition of variables are provided in Table 3.

Parameter	Definition
γ^j	relative risk aversion
ρ^j	discount rate
ζ^j	intertemporal elasticity of substitution
μ^a	growth rate of capital
σ^a	volatility of capital
μ^O	sentiment factor
α^a	productivity
κ	investment cost

Table 2: Constant Parameters

Type	Definition
State Variables	$\eta_t (\eta)$
Agents	ξ_t^i, ξ_t^h
Endogenous Variables	$\mu_t^\eta, \sigma_t^{\eta^a}, q_t^a, w_t^{ia}, w_t^{ha}$

Table 3: Variables

Equations:

$$\iota_t^a = \frac{q_t^a - 1}{\kappa} \quad (42)$$

$$\Phi(\iota_t^a) = \frac{1}{\kappa} \log(1 + \kappa \iota_t^a) \quad (43)$$

$$c_t^j = (\rho^j)^{\zeta^j} (\xi_t^j)^{1-\zeta^j} \quad (44)$$

$$\sigma_t^{qa} = \frac{1}{q_t^a} \frac{\partial q_t^a}{\partial \eta_t} \sigma_t^{\eta^a} \eta_t \quad (45)$$

$$\sigma_t^{nja} = w_t^{ja} (\sigma^a + \sigma_t^{qa}) \quad (46)$$

$$\sigma_t^{\xi ja} = \frac{1}{\xi_t^j} \frac{\partial \xi_t^j}{\partial \eta_t} \sigma_t^{\eta^a} \eta_t \quad (47)$$

$$\sigma_t^{na} = \eta_t \sigma_t^{nia} + (1 - \eta_t) \sigma_t^{nha} \quad (48)$$

$$\mu_t^{qa} = \frac{1}{q_t^a} \left(\frac{\partial q_t^a}{\partial \eta_t} \mu_t^\eta \eta_t + \frac{1}{2} \frac{\partial^2 q_t^a}{\partial \eta_t^2} (\sigma_t^{\eta^a} \eta_t)^2 \right) \quad (49)$$

$$r_t^{ka} = \mu_t^{qa} + \mu^a + \Phi_t^a + \sigma^a \sigma^{qa} + \frac{\alpha^a - \iota_t^a}{q_t^a} \quad (50)$$

$$r_t = r_t^{ka} - \gamma^h w_t^{ha} (\sigma^a + \sigma_t^{qa})^2 + (1 - \gamma^h) \sigma_t^{\xi ha} (\sigma^a + \sigma_t^{qa}) \quad (51)$$

$$\mu_t^{nj} = r_t - c_t^j + w_t^{ja} (r_t^{ka} - r_t) \quad (52)$$

$$\mu_t^{\xi j} = \frac{1}{\xi_t^j} \left(\frac{\partial \xi_t^j}{\partial \eta_t} \mu_t^\eta \eta_t + \frac{1}{2} \frac{\partial^2 \xi_t^j}{\partial \eta_t^2} (\sigma_t^{\eta^a} \eta_t)^2 \right) \quad (53)$$

$$r_t^{\hat{ka}} = r_t^{ka} + \frac{\mu^O - \mu^a}{\sigma^a} (\sigma^a + \sigma_t^{qa}) \quad (54)$$

Endogenous equations:

$$\mu_t^\eta = (1 - \eta_t) (\mu_t^{ni} - \mu_t^{nh}) + (\sigma_t^{na})^2 - \sigma_t^{nia} \sigma_t^{na} \quad (55)$$

$$\sigma_t^{\eta^a} = (1 - \eta_t) (\sigma_t^{nia} - \sigma_t^{nha}) \quad (56)$$

$$r_t^{\hat{ka}} - r_t = \gamma^i w_t^{ia} (\sigma^a + \sigma_t^{qa})^2 - (1 - \gamma^i) \sigma_t^{\xi ia} (\sigma^a + \sigma_t^{qa}) \quad (57)$$

$$1 = w_t^{ia} \eta_t + w_t^{ha} (1 - \eta_t) \quad (58)$$

$$\alpha^a - \iota_t^a = (c_t^i \eta_t + c_t^h (1 - \eta_t)) q_t^a \quad (59)$$

HJB equations:

$$\begin{aligned} & \frac{\rho^i}{1 - \frac{1}{\zeta^i}} \left(\left(\frac{c_t^i}{\xi_t^i} \right)^{1-1/\zeta^i} - 1 \right) + \mu_t^{\xi i} + \mu_t^{ni} \\ & - \frac{\gamma^i}{2} (\sigma_t^{nia})^2 - \frac{\gamma^i}{2} (\sigma_t^{\xi ia})^2 + (1 - \gamma^i) \sigma_t^{\xi ia} \sigma_t^{nia} \end{aligned} \quad (60)$$

$$\begin{aligned} & \frac{\rho^h}{1 - \frac{1}{\zeta^h}} \left(\left(\frac{c_t^h}{\xi_t^h} \right)^{1-1/\zeta^h} - 1 \right) + \mu_t^{\xi h} + \mu_t^{nh} \\ & - \frac{\gamma^h}{2} (\sigma_t^{nha})^2 - \frac{\gamma^h}{2} (\sigma_t^{\xi ha})^2 + (1 - \gamma^h) \sigma_t^{\xi ha} \sigma_t^{nha} \end{aligned} \quad (61)$$

B Log Utility Model

This appendix presents Proposition 4 from [1] and PyMacroFin 1D example, which is replicated in Section 4.4. The state variable is η and $q(\eta)$ is an unknown price function. The goal is to compute $\psi(\eta)$ and η^ψ . ψ has the property: $\psi(\eta) < 1$ on $[0, \eta^\psi)$, and $\psi(\eta) = 1$ on $[\eta^\psi, 1]$. These variables should satisfy:

$$(r(1 - \eta) + \rho\eta)q = \psi a + (1 - \psi)\underline{a} - \iota. \quad (62)$$

σ_t^q and law of motion of η are given by

$$\sigma + \sigma_t^q = \sqrt{\frac{a - \underline{a}/q + \underline{\delta} - \delta}{\psi/\eta - (1 - \psi)/(1 - \eta)}} \quad (63)$$

$$\frac{\partial q}{\partial \eta} = \frac{q}{\psi - \eta} \left(1 - \frac{\sigma}{\sigma + \sigma_t^q} \right) \quad (64)$$

$$\sigma_t^\eta = \frac{\psi - \eta}{\eta} (\sigma + \sigma_t^q) \quad (65)$$

$$\mu_t^\eta = (\sigma_t^\eta)^2 + \frac{a - \iota}{q} + (1 - \psi)(\underline{\delta} - \delta) - \rho \quad (66)$$

Following [1] and PyMacroFin, the constants for this model are $\rho = 0.06$, $r = 0.05$, $a = 0.11$, $\underline{a} = 0.07$, $\delta = \underline{\delta} = 0.05$, $\sigma = 0.1$, $\kappa = 2$.

The initial function guesses are from PyMacroFin:

$$q = \begin{cases} 1.05 + 0.06/0.3\eta, & \eta < 0.3 \\ 1.1 - 0.03/0.7\eta, & \eta \geq 0.3 \end{cases} \quad (67)$$

$$\psi = \begin{cases} 1/0.3\eta, & \eta < 0.3 \\ 1, & \eta \geq 0.3 \end{cases} \quad (68)$$

A single initial condition $q(0) = \sqrt{2\underline{a}\kappa + (\kappa r)^2 + 1} - \kappa r$ is used.

We rewrite the equations defining σ_t^q , and use the following equations and endogenous equations for training the model, with an additional constraint $\psi \leq 1$.

Equations:

$$\iota = \frac{q^2 - 1}{2\kappa} \quad (69)$$

$$\sigma_t^q = \frac{\sigma}{1 - \frac{1}{q} \frac{\partial q}{\partial \eta} (\psi - \eta)} - \sigma \quad (70)$$

$$\sigma_t^\eta = \frac{\psi - \eta}{\eta} (\sigma + \sigma_t^q) \quad (71)$$

$$\mu_t^\eta = (\sigma_t^\eta)^2 + \frac{a - \iota}{q} + (1 - \psi)(\underline{\delta} - \delta) - \rho \quad (72)$$

Endogenous equations:

$$(r(1 - \eta) + \rho\eta)q = \psi a + (1 - \psi)\underline{a} - \iota \quad (73)$$

$$(\sigma + \sigma_t^q)^2 (\psi/\eta - (1 - \psi)/(1 - \eta)) = \frac{a - \underline{a}}{q} + \underline{\delta} - \delta \quad (74)$$

Note that for (73), we can enforce the condition of $\psi = 1$ and $\psi < 1$ using constraint-activated systems:

$$(r(1 - \eta) + \rho\eta)q = \psi a + (1 - \psi)\underline{a} - \iota, \text{ if } \psi < 1 \quad (75)$$

$$(r(1 - \eta) + \rho\eta)q = a - \iota, \text{ if } \psi \geq 1 \quad (76)$$

C Stochastic Volatility Model (Di Tella 2017)

In this section, we replicate the results for the 2D model proposed in [2]. We restate key components of the model essential for solving the problem and refer readers to the original paper for further details. Similar to Section A, there are two types of agents: experts (intermediary) who can trade and use capital to produce and households that finance them. Capital is exposed to both aggregate and (expert-specific) idiosyncratic Brownian TFP shocks. The change in expert's effective capital in a short period of time is

$$\frac{dk_t}{k_t} = g_t dt + \sigma dZ_t + v_t dW_t, \quad (77)$$

where g_t is the growth rate for the capital stock, $\iota(g)$ is the investment function, Z is an aggregate Brownian motion, and W is an idiosyncratic Brownian motion for expert in a probability space $(\Omega, \mathcal{F}_t, \mathcal{P})$. The exposure of capital to aggregate risk $\sigma > 0$ is constant, but the exposure to idiosyncratic risk v_t follows an exogenous stochastic process,

$$dv_t = \lambda(\bar{v} - v_t)dt + \bar{\sigma}_v \sqrt{v_t} dZ_t, \quad (78)$$

where \bar{v} is the long-run mean and λ is the mean reversion parameter. The loading of the idiosyncratic volatility of capital on aggregate risk is $\bar{\sigma}_v < 0$, so Z is an aggregate shock that increases the effective capital stock and reduces idiosyncratic risk. This v_t extends the dimensionality of the economic model to two.

Both experts and households have Epstein-Zin preferences with the same discount rate ρ , risk aversion γ , and elasticity of intertemporal substitution (EIS) ψ^{-1} . The utility function is given as

$$U_t^j = \mathbb{E}_t \left[\int_t^\infty f(c_s, U_s) ds \right], \quad (79)$$

where the normalized aggregator of consumption and continuation value is

$$f(c, U) = \frac{1}{1-\psi} \left(\frac{\rho c^{1-\psi}}{[(1-\gamma)U]^{(\gamma-\psi)/(1-\gamma)}} - \rho(1-\gamma)U \right). \quad (80)$$

Experts trade capital continuously at price p , whose process can be conjectured as:

$$\frac{dp_t}{p_t} = \mu_{p,t} dt + \sigma_{p,t} dZ_t. \quad (81)$$

The total value of the aggregate capital stock is $p_t k_t$, and it constitutes the total wealth of the economy. The financial market has stochastic discount factor η with:

$$\frac{d\eta_t}{\eta_t} = -r_t dt - \pi_t dZ_t, \quad (82)$$

where r_t is the risk-free interest rate and π_t is the price of aggregate risk Z .

The cumulative return from investing a dollar in capital for expert is R_t^k , with

$$dR_t^k = \left(\frac{a - \iota(g_t)}{p_t} + g_t + \mu_{p,t} + \sigma \sigma_{p,t} \right) dt + (\sigma + \sigma_{p,t}) dZ_t + v_t dW_t. \quad (83)$$

Experts solve the following optimization problem:

$$\max_{e, g, k, \theta} U(e) \quad (84)$$

$$\text{subject to } \frac{dn_t}{n_t} = (\mu_{n,t} - \hat{e}_t) dt + \sigma_{n,t} dZ_t + \tilde{\sigma}_{n,t} dW_t, \quad (85)$$

where n is the expert's net worth, $\sigma_{n,t}$ is their exposure to aggregate risk, and $\tilde{\sigma}_{n,t}$ is their exposure to idiosyncratic risk. $\tilde{\sigma}_{n,t}$ comes from the fraction $\phi \in (0, 1)$ (moral hazard) of their return that they keeps. They sells the rest of $1 - \phi$ on the market. θ is expert's position in the normalized market index.

The value function for an expert with net worth n is

$$V(n) = \frac{(\xi_t n)^{1-\gamma}}{1-\gamma}, \quad (86)$$

for some stochastic process ξ_t such that

$$\frac{d\xi_t}{\xi_t} = \mu_{\xi,t}dt + \sigma_{\xi,t}dZ_t. \quad (87)$$

The experts retire with independent Poisson arrival rate $\tau > 0$ and become households. The turnover gives a modified HJB equation for experts:

$$\frac{\rho}{1-\psi} = \max \left\{ \frac{\hat{e}^{1-\psi}}{1-\psi} \rho \xi^{\psi-1} + \frac{\tau}{1-\gamma} \left(\left(\frac{\xi}{\xi} \right)^{1-\gamma} - 1 \right) + \mu_n - \hat{e} + \mu_\xi - \frac{\gamma}{2} \left(\sigma_n^2 + \sigma_\xi^2 - 2 \frac{1-\gamma}{\gamma} \sigma_n \sigma_\xi + \tilde{\sigma}_n^2 \right) \right\}. \quad (88)$$

Households solve the following optimization problem:

$$\max_{c, \sigma_w} U(c) \quad (89)$$

$$\text{subject to } \frac{dw_t}{w_t} = (r_t + \sigma_{w,t}\pi_t - \hat{c}_t)dt + \sigma_{w,t}dZ_t, \quad (90)$$

where w is the wealth of households, and $\sigma_{w,t}$ is their exposure to aggregate risk.

The value function for a household with net wealth w is

$$V(w) = \frac{(\zeta_t w)^{1-\gamma}}{1-\gamma}, \quad (91)$$

for some stochastic process ζ_t such that

$$\frac{d\zeta_t}{\zeta_t} = \mu_{\zeta,t}dt + \sigma_{\zeta,t}dZ_t. \quad (92)$$

The HJB equation associated with households' problem is

$$\frac{\rho}{1-\psi} = \max \left\{ \frac{\hat{c}^{1-\psi}}{1-\psi} \rho \zeta^{\psi-1} + \mu_w - \hat{c} + \mu_\zeta - \frac{\gamma}{2} \left(\sigma_w^2 + \sigma_\zeta^2 - 2 \frac{1-\gamma}{\gamma} \sigma_w \sigma_\zeta \right) \right\}. \quad (93)$$

The state space is defined by two state variables: $x = n/pk$, representing the net worth of experts relative to the total value of assets in equilibrium; and v , indicating the experts' exposure to idiosyncratic risk. $(x, v) \in (0, 1) \times (0, \infty)$.

Market clearing condition at equilibrium gives the following conditions:

$$\begin{aligned} a - \iota &= p(\hat{e}x + \hat{c}(1-x)) \\ \sigma + \sigma_p &= \sigma_n x + \sigma_w(1-x) \\ \frac{a - \iota}{p} + g + \mu_p + \sigma \sigma_p - r &= (\sigma + \sigma_p)\pi + \gamma \frac{1}{x} (\phi v)^2 \end{aligned}$$

C.1 Model Details

The model adheres to the replication package provided by [2]. The investment function $\iota(g)$ is specified quadratically, with parameters selected to ensure that the annualized average growth rate of GDP is 2% and the average investment to GDP ratio is 20%. We need to parametrize r because it depends on unknown μ_ξ . However, π can be computed explicitly using known variables and thus does not require parameterization. The definitions of constant parameters are provided in Table 4 and the definitions of variables are provided in Table 5.

Equations:

$$\begin{aligned} g &= \frac{1}{2A}(p - B) - \delta \\ \iota &= A(g + \delta)^2 + B(g + \delta) \\ \mu_v &= \lambda(\bar{v} - v) \\ \sigma_v &= \bar{\sigma}_v \sqrt{v} \end{aligned}$$

Parameter	Definition	Value
a	relative risk aversion	$a = 1$
σ	volatility of TFP shocks	$\sigma = 0.0125$
λ	mean reversion coefficient for idiosyncratic risk	$\lambda = 1.38$
\bar{v}	long-run mean of idiosyncratic risk	$\bar{v} = 0.25$
$\bar{\sigma}_v$	idiosyncratic volatility of capital on aggregate risk	$\bar{\sigma}_v = -0.17$
ρ	discount rate	$\rho = 0.0665$
γ	risk aversion rate	$\gamma = 5$
ψ	inverse of elasticity of intertemporal substitution	$\psi = 0.5$ s.t. EIS=2
τ	Poisson retirement rate for experts	$\tau = 1.15$
ϕ	moral hazzard	$\phi = 0.2$
A	second order coefficient for investment function	$A = 53$
B	first order coefficient for investment function	$B = -0.8668571428571438$
δ	shift for investment function	$\delta = 0.05$

Table 4: Di Tella 2017 Constant Parameters

Type	Definition
State Variables	$(x, v) \in [0.05, 0.95] \times [0.05, 0.95]$
Agents	ξ (experts), ζ (households)
Endogenous Variables	p (price), r (risk-free rate)

Table 5: Di Tella 2017 Variables

$$\begin{aligned}
\hat{e} &= \rho^{1/\psi} \xi^{(\psi-1)/\psi} \\
\hat{c} &= \rho^{1/\psi} \zeta^{(\psi-1)/\psi} \\
\sigma_{x,1} &= (1-x)x \frac{1-\gamma}{\gamma} \left(\frac{1}{\xi} \frac{\partial \xi}{\partial v} - \frac{1}{\zeta} \frac{\partial \zeta}{\partial v} \right) \\
\sigma_{x,2} &= 1 - (1-x)x \frac{1-\gamma}{\gamma} \left(\frac{1}{\xi} \frac{\partial \xi}{\partial x} - \frac{1}{\zeta} \frac{\partial \zeta}{\partial x} \right) \\
\sigma_x &= \frac{\sigma_{x,1}}{\sigma_{x,2}} \sigma_v \\
\sigma_p &= \frac{1}{p} \left(\frac{\partial p}{\partial v} \sigma_v + \frac{\partial p}{\partial x} \sigma_x \right) \\
\sigma_\xi &= \frac{1}{\xi} \left(\frac{\partial \xi}{\partial v} \sigma_v + \frac{\partial \xi}{\partial x} \sigma_x \right) \\
\sigma_\zeta &= \frac{1}{\zeta} \left(\frac{\partial \zeta}{\partial v} \sigma_v + \frac{\partial \zeta}{\partial x} \sigma_x \right) \\
\sigma_n &= \sigma + \sigma_p + \frac{\sigma_x}{x} \\
\pi &= \gamma \sigma_n + (\gamma - 1) \sigma_\xi \\
\sigma_w &= \frac{\pi}{\gamma} - \frac{\gamma - 1}{\gamma} \sigma_\zeta \\
\mu_w &= r + \pi \sigma_w \\
\mu_n &= r + \frac{\gamma}{x^2} (\phi v)^2 + \pi \sigma_n \\
\tilde{\sigma}_n &= \frac{\phi}{x} v \\
\mu_x &= x \left(\mu_n - \hat{e} - \tau + \frac{a - \iota}{p} - r - \pi(\sigma + \sigma_p) - \frac{\gamma}{x} (\phi v)^2 + (\sigma + \sigma_p)^2 - \sigma_n(\sigma + \sigma_p) \right) \\
\mu_p &= \frac{1}{p} \left(\mu_v \frac{\partial p}{\partial v} + \mu_x \frac{\partial p}{\partial x} + \frac{1}{2} \left(\sigma_v^2 \frac{\partial^2 p}{\partial v^2} + 2\sigma_v \sigma_x \frac{\partial^2 p}{\partial v \partial x} + \sigma_x^2 \frac{\partial^2 p}{\partial x^2} \right) \right)
\end{aligned}$$

$$\begin{aligned}\mu_\xi &= \frac{1}{\xi} \left(\mu_v \frac{\partial \xi}{\partial v} + \mu_x \frac{\partial \xi}{\partial x} + \frac{1}{2} \left(\sigma_v^2 \frac{\partial^2 \xi}{\partial v^2} + 2\sigma_v \sigma_x \frac{\partial^2 \xi}{\partial v \partial x} + \sigma_x^2 \frac{\partial^2 \xi}{\partial x^2} \right) \right) \\ \mu_\zeta &= \frac{1}{\zeta} \left(\mu_v \frac{\partial \zeta}{\partial v} + \mu_x \frac{\partial \zeta}{\partial x} + \frac{1}{2} \left(\sigma_v^2 \frac{\partial^2 \zeta}{\partial v^2} + 2\sigma_v \sigma_x \frac{\partial^2 \zeta}{\partial v \partial x} + \sigma_x^2 \frac{\partial^2 \zeta}{\partial x^2} \right) \right)\end{aligned}$$

Endogenous equations:

$$\begin{aligned}a - \iota &= p(\hat{e}x + \hat{c}(1-x)) \\ \sigma + \sigma_p &= \sigma_n x + \sigma_w(1-x) \\ \frac{a - \iota}{p} + g + \mu_p + \sigma \sigma_p - r &= (\sigma + \sigma_p)\pi + \gamma \frac{1}{x}(\phi v)^2\end{aligned}$$

HJB equations:

$$\begin{aligned}\frac{\hat{e}^{1-\psi}}{1-\psi} \rho \xi^{\psi-1} + \frac{\tau}{1-\gamma} \left(\left(\frac{\zeta}{\xi} \right)^{1-\gamma} - 1 \right) + \mu_n - \hat{e} + \mu_\xi - \frac{\gamma}{2} \left(\sigma_n^2 + \sigma_\xi^2 - 2 \frac{1-\gamma}{\gamma} \sigma_n \sigma_\xi + \tilde{\sigma}_n^2 \right) - \frac{\rho}{1-\psi} \\ \frac{\hat{c}^{1-\psi}}{1-\psi} \rho \zeta^{\psi-1} + \mu_w - \hat{c} + \mu_\zeta - \frac{\gamma}{2} \left(\sigma_w^2 + \sigma_\zeta^2 - 2 \frac{1-\gamma}{\gamma} \sigma_w \sigma_\zeta \right) - \frac{\rho}{1-\psi}\end{aligned}$$

C.2 Results

The agent wealth multipliers (ξ , ζ) and endogenous variables (p , r) are configured as 4-layer MLPs with 30 hidden units per layer and tanh activation. ξ , ζ , and p are constrained by SoftPlus to ensure positive outputs, thereby guaranteeing that the price of capital and agent wealth remain non-negative. The system is trained on a 50×50 equispaced fixed grid on $[0.05, 0.95] \times [0.05, 0.95]$ for 10000 epochs using Adam optimizer with a learning rate of 10^{-3} , under the endogenous and HJB constraints. Figure 7 and 8 replicate Fig. 1 and 2 from the original paper respectively. There are some regions (specifically $v \in [0.25, 0.6]$), where the functions do not behave as expected. Residual-based Adaptive Refinements (RAR) and active learning can be applied to improve the approximations [5, 6, 4]. However, these refinements are not the focus of the current iteration of work, and the results are therefore not included.

D Online Resources

The Deep-MacroFin code repository is available at <https://github.com/rotmanfinhub/deep-macrofin>. Documentation and more examples are available in the code repository and at <https://rotmanfinhub.github.io/deep-macrofin>.

References

- [1] Markus K. Brunnermeier and Yuliy Sannikov. “A Macroeconomic Model with a Financial Sector”. In: *American Economic Review* 104.2 (Feb. 2014), pp. 379–421. DOI: 10.1257/aer.104.2.379. URL: <https://www.aeaweb.org/articles?id=10.1257/aer.104.2.379>.
- [2] Sebastian Di Tella. “Uncertainty Shocks and Balance Sheet Recessions”. In: *Journal of Political Economy* 125.6 (2017), pp. 2038–2081. DOI: 10.1086/694290. eprint: <https://doi.org/10.1086/694290>. URL: <https://doi.org/10.1086/694290>.
- [3] Larry G. Epstein and Stanley E. Zin. “Substitution, Risk Aversion, and the Temporal Behavior of Consumption and Asset Returns: A Theoretical Framework”. In: *Econometrica* 57.4 (1989), pp. 937–969. ISSN: 00129682, 14680262. URL: <http://www.jstor.org/stable/1913778> (visited on 06/30/2024).
- [4] Goutham Gopalakrishna. *ALIENS and Continuous Time Economies*. Swiss Finance Institute Research Paper Series 21-34. Swiss Finance Institute, 2021. URL: <https://EconPapers.repec.org/RePEc:chf:rpseri:rp2134>.
- [5] Lu Lu et al. “DeepXDE: A Deep Learning Library for Solving Differential Equations”. In: *SIAM Review* 63.1 (2021), pp. 208–228. DOI: 10.1137/19M1274067. eprint: <https://doi.org/10.1137/19M1274067>. URL: <https://doi.org/10.1137/19M1274067>.
- [6] Chenxi Wu et al. “A comprehensive study of non-adaptive and residual-based adaptive sampling for physics-informed neural networks”. In: *Computer Methods in Applied Mechanics and Engineering* 403 (Jan. 2023), p. 115671. ISSN: 0045-7825. DOI: 10.1016/j.cma.2022.115671. URL: <http://dx.doi.org/10.1016/j.cma.2022.115671>.

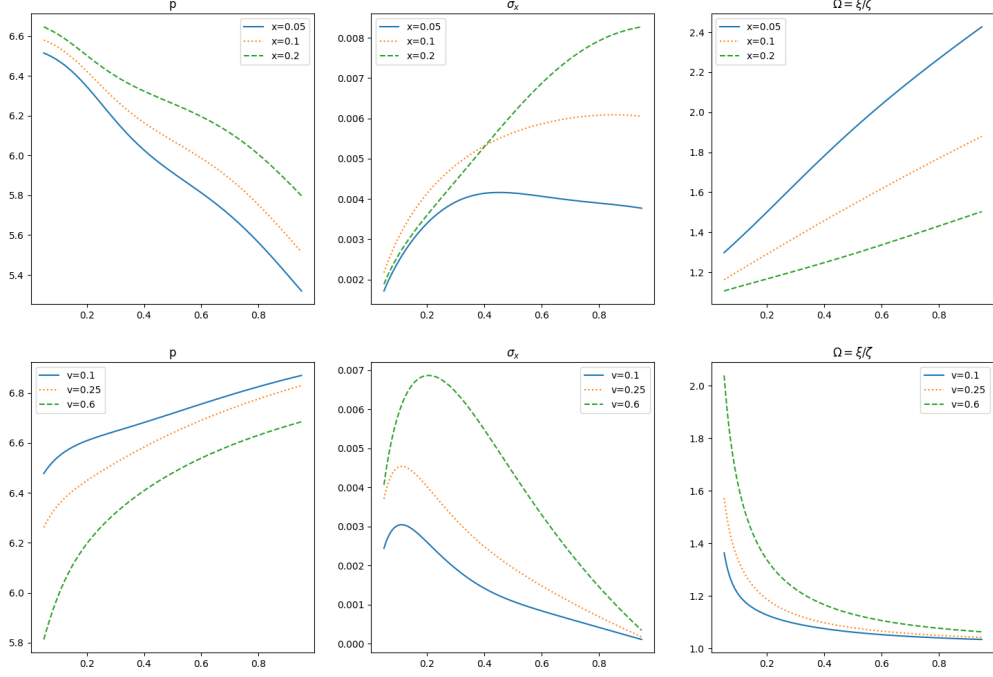


Figure 7: The price of capital p , volatility of x , σ_x , and relative investment opportunities $\Omega = \xi/\zeta$, as functions of v (above) for $x = 0.05$ (blue solid), $x = 0.1$ (orange dotted), and $x = 0.2$ (green dashed), and as functions of x (below) for $x = 0.1$ (blue solid), $x = 0.25$ (orange dotted), and $x = 0.6$ (green dashed).

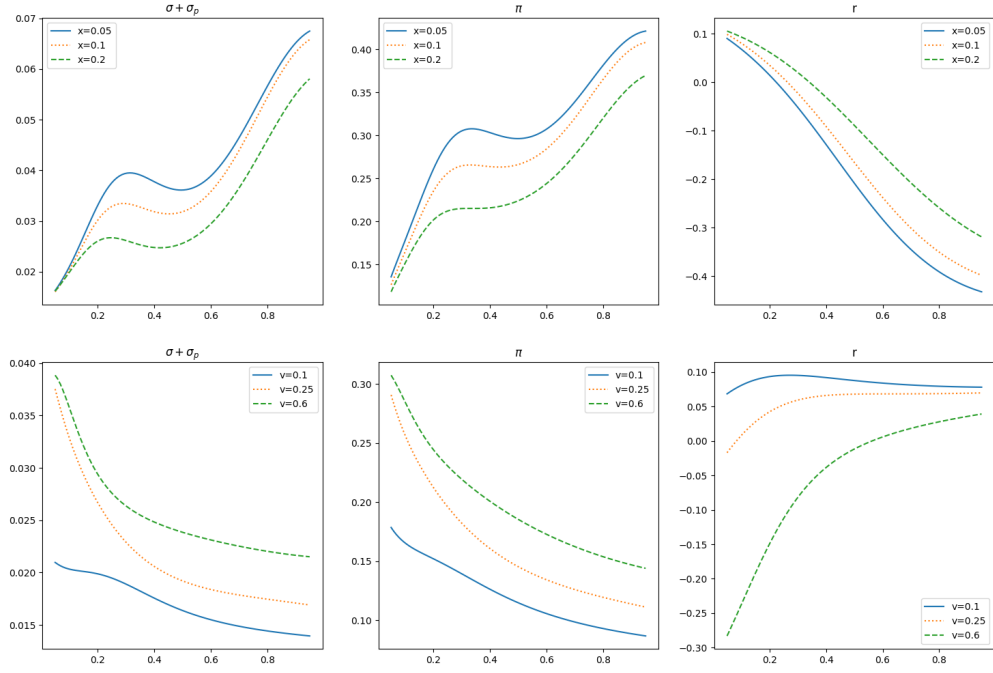


Figure 8: Aggregate risk $\sigma + \sigma_p$, the price of risk π , and the risk-free rate r , as functions of v (above) for $x = 0.05$ (blue solid), $x = 0.1$ (orange dotted), and $x = 0.2$ (green dashed), and as functions of x (below) for $x = 0.1$ (blue solid), $x = 0.25$ (orange dotted), and $x = 0.6$ (green dashed).